Strategies to Maximize the Wood Production in Amazon Forest

Aline Canetti
Independent forest consultant
Evaldo Muñoz Braz
Embrapa Florestas
Patricia Mattos (patricia.mattos@embrapa.br)
Embrapa Florestas https://orcid.org/0000-0003-4134-8890
Renato Olivir Basso
Elabore Projetos e Consultoria Florestal
Afonso Figueiredo Filho
UNICENTRO: Universidade Estadual do Centro-Oeste

Research

Keywords: dendrochronology, forest modeling, minimum cutting diameter

Posted Date: October 1st, 2020

DOI: https://doi.org/10.21203/rs.3.rs-83620/v1

TITLE PAGE

Strategies to maximize the wood production in Amazon forest

Aline Canetti[1], Evaldo Muñoz Braz[2], Patrícia Póvoa de Mattos[2*], Renato Olivir Basso[3], Afonso Figueiredo Filho[4]

(Canetti, A., Braz, E. M., Mattos, P. P., Basso, R. O., Figueiredo Filho, A.)

*Corresponding author: patricia.mattos@embrapa.br, +55 41 3675-5625 fax: +55 41 3675-5600

[1]Independent forestry consultant; E-mail: alinecanetti@gmail.com

[2]Embrapa Florestas. Estrada da Ribeira Km 111, Caixa Postal 319. 83411-000, Colombo, PR, Brazil; E-mail: evaldo.braz@embrapa.br; patricia.mattos@embrapa.br

[3]Elabore Projetos e Consultoria Florestal. Av. Gov. Júlio Campos, 207 - St. Comercial. 78550-000, Sinop, Brazil; E-mail: elabore@terra.com.br

[4]Universidade Estadual do Centro-Oeste. PR 153, Km 7, s/n - Riozinho, Irati, PR, Brazil. 84500-000. E-mail: afigfilho@gmail.com

To the Editor-in-Chief:

Dear Sir,

We would like to submit the manuscript “Strategies to maximize the wood production in Amazon forest” to possible publication in the Forest Ecosystems Journal, we strongly believe our theme fits within its scope.

We confirm that the manuscript was not published or it is not under evaluation elsewhere in substantially the same or abbreviated form, either in print or electronically.

The innovation of this paper was the use of the analysis of the original structure of the forest combined with growth models to predict the optimal wood production in Amazon forest. It may be used by forest managers and forest law-makers, aiming to maximize sustainable wood production in the Amazon Forest.

Forest Ecology and Management was the most cited journal in our paper and

Sincerelly,

Patrícia Póvoa de Mattos

Strategies to maximize the wood production in Amazon forest

ABSTRACT

Background: This study aimed to develop a procedure to determine which logging diameter would achieve optimal wood production by species, aiming to support sustainable management of the Amazon forest. Two main methodologies of analysis by species were combined: probability density function (PDF) and growth modeling. The growth models were used to derive the volume increment curves at the individual tree level. To detect the points of maximum annual increment in volume at the population tree level we used PDF with adjusted growth equations.

Results: The population maximum annual volumetric increments occurred in smaller diameters compared to that of the individual-level. When combining shorter cutting cycles with the population biological rotation point considered as the minimum cutting diameter (MCD), we observed higher annual increments in volume than that achieved using the Brazilian law criteria (MCD = 50 cm) or other MCD tested.

Conclusion: The procedure proposed may be used by forest managers and forest law-makers, aiming to maximize sustainable wood production in the Amazon forest.

Keywords: dendrochronology; forest modeling; minimum cutting diameter

Background

Natural forests are steadily accumulating biomass, reflected in the production of carbon and wood. The forest functions must be maintained after logging, and the remaining stocks must allow a continuous production of wood for the next interventions, ensuring forest management sustainability (Ong; Kleine, 1996; Van Gardingen et al., 2006; Braz et al., 2015; Avila et al., 2017). The management must be carefully planned and be

consistent with the initial natural forest structure (e.g., density, diametric distribution, growth, mortality, and regeneration) of the species of interest (Seydack et al., 1995; Bick et al., 1998).

According to Seydack (2012), a challenge for forestry scientists is to combine modeling and simulation tools to understand tropical forest dynamics, enabling production maximization. Minimum cutting diameters (MCD) should be defined for all commercial species, representing a powerful tool in maximizing increment for tropical forests under management as in the Amazon region.

Knowledge of the natural forest balance allows identification of the ideal moment of intervention and its production potential (Bick et al., 1998). The forest balance equation depends on how tree increment occurs over time. Studies of species growth at individual-level, structure, and reproductive biology are the basis for defining the management guidelines that guarantee sustainability for wood production in tropical forests (Vanclay, 1989; Miranda, D. L. C. et al., 2018; Dionisio et al., 2018).

Forest growth goes through youth, maturity, senescence, and stagnation phases. Its basic unit is the tree, which has a distinct sigmoidal growth pattern, tending to a biological limit (Odum, 1988). Trees that were established decades ago will grow within the ingress criteria for classes with larger diameters, will stagnate or eventually die. Thus, a diametric distribution of natural forest is the result of several tree establishments over different periods.

Diametric distribution is a useful factor to describe the forest properties since the diameter is easily obtained and correlated with other variables such as volume, which defines the economic value of the forest area (Bailey; Dell, 1973). Diameter is widely used in the forest sector to assess the effect of environmental and anthropogenic disturbances (Kohyama, 1986; Coomes et al., 2003; Wright et al., 2003; Bettinger et al.,

2009; Hossain et al., 2015), to describe successional patterns (Kohyama, 1986; Wright et al., 2003; Wang et al., 2009) and for the prediction of the future stock of a stand (De Liocourt, 1898; Meyer, 1952; Carvalho, 1981; Condit et al. , 1998; Bettinger et al., 2009; Hossain et al., 2015; Orellana; Figueiredo Filho, 2017). However, future stock projection is difficult for tropical forest due to its great diversity (Orellana, Figueiredo Filho, 2017). Moreover, information about individual species distribution pattern is scarce.

Describing forest growth trajectory requires long-term information when permanent plots are used as data source (Bick et al., 1998). The successive measurements can make it difficult or even imply a failed simulation, due to the time spent to replicate a structure that represents the initial diametric classes up to the biological diameter limit of the species (Brienen; Zuidema, 2006a; Miranda D. L. C. et al., 2018).

Most studies of the species forest growth in the Amazon basin were carried out with permanent plots (Silva, 1989; 1997; Higuchi, 1996; Fortini et al., 2015; Avila et al., 2017; D'Oliveira et al., 2017) and supported the management guidelines in the Brazilian legislation (Silva, 1989, 1997; Higuchi, 1996). However, in some species less than one individual per hectare occurs in Amazonian primary forest structure, especially when considering trees with commercial dimensions (Miranda, D. L. C. et al., 2018), and extensive sample areas are therefore required to properly represent a population of individual species (Groenendijk et al., 2017; Miranda, D. L. C. et al., 2018.).

In addition to area size, time scale is also a limiting factor in studying forest dynamics with permanent plots (Brienen; Zuidema, 2006a; Miranda, D. L. C. et al., 2018). In Brazil, permanent plots monitored for more than 40 years are rare. These periods are short compared to the age of commercial trees, which are rarely less than 100 years old (Brienen; Zuidema, 2006a; Schöngart, 2008; Rosa et al., 2017).

Growth series obtained by dendrochronology became more popular as an alternative to permanent-plot data to supply the demand for information and growth models of species (Brienen, 2005; Brienen; Zuidema, 2006a; Schöngart, 2011; Mattos et al., 2015; Canetti et al., 2017; Groenendijk et al., 2017; Miranda, D. L. C. et al., 2018). Growth ring analysis is a fast and reliable tool for assessing tree age, determining its growth rates over the life cycle, and identifying growth differences between species (Groenendijk et al., 2017; Rosa et al., 2017).

This study aimed to develop a procedure based on the diametric structure and growth models to set the minimum cutting diameter (MCD) for optimal wood production. The procedure was tested on four species in the Brazilian Amazon. The results may be used as a basis for forest management plans and to aid in the revision and modernization of forest law in countries with humid tropical forests.

Methods

This study was conducted in the Sinop micro-region (11°50 S; 54°50' W), Mato Grosso (MT) state, within the Brazilian Legal Amazon. The region comprises 9 municipalities, encompassing nearly 40 thousand km² (IBGE, 2010). The region's vegetation is characterized by a transition zone between open tropical rainforest and deciduous tropical rainforest, and is the largest area composed of this ecotone in the world (IBGE 1992; SIVAM 2002). The micro-region presents flat relief and tropical climate with a dry season between autumn and winter (Alvares et al., 2013). All compartments from which data were collected were included in sustainable forest management plans authorized by the State Environmental Agency (SEMA-MT).

The species *Apuleia leiocarpa* (Vogel) J.F. Macbr., *Erisma uncinatum* Warm., *Hymenolobium excelsum* Ducke, and *Trattinnickia burserifolia* Mart. were studied.

Together, these species represent 25% of the commercial volume logged in the micro-region of Sinop, the second-largest tropical wood production hub in Brazil (Ribeiro et al., 2016).

Fitting probability density function of the diametric structure of species

The data were obtained from 100% inventories of six forest compartments carried out in the municipalities of Santa Carmem, Sinop, and União do Sul, totaling 5,432 ha. Forest inventories were conducted from 2011 to 2014, by measuring all trees with diameter at 1.30 m above ground level (dbh) ≥ 40 cm (n = 3,617 for *A. leiocarpa*, 13,655 for *E. uncinatum*, 1,814 for *H. excelsum*, and 16,162 for *T. burserifolia*).

Data from sample units of 0.25 ha (10 m x 250 m) were also used to complement the densities of the smaller diameter trees (20 ≤ dbh ≤ 40 cm), not covered in the 100% inventories. These plots were measured in four compartments in the municipalities of Santa Carmem and Feliz Natal, MT. All trees with dbh ≥ 20 cm were measured. Altogether, data from 138 plots were used, adding up to 36 ha inventoried. On average, there were 35 trees ha^{-1} with 20 ≤ dbh <40 cm (5 of *A. leiocarpa*, 11 of *E. uncinatum*, 4 of *H. excelsum*, and 121 of *T. burserifolia*).

The dbh data for each species were grouped into diametric classes of 10 cm-range to fit probability density functions (PDFs). Normal, Beta, Gamma, Log-Normal, Johnson's SB, and Weibull with three parameters (Scolforo, 1998) PDFs were fitted. The diametric structure of each species included the largest diameter class in which live individuals were found in the 100% inventories. To avoid total numbers of individuals less than one tree per ha per species (as occurred for *A. leiocarpa* and *H. excelsum*), the densities of individuals were considered on a 10-ha scale (i.e. number of trees 10 ha^{-1}).

The goodness-of-fit tests of PDFs by species were performed in two steps, using the Kolmogorov-Smirnov test ($\alpha = 0.05$). Initially, the goodness-of-fit of the theoretical

126 PDFs to the empirical data was tested in each forest compartment. In the second stage,
127 the goodness-of-fit of the PDFs fitted to the data of the entire Sinop micro-region (i.e.,
128 for the total data set) were tested considering sample inventories and 100% inventories.
129 The best PDF for each species was selected based on the lowest maximum absolute
130 value between theoretical PDF and observed data ($D_{calc.}$ For Kolmogorov-Smirnov test)
131 and lowest error index (Reynolds et al., 1988).

132 **Modeling diametric growth by species**

133 Stem sections (discs) with approximately 5-cm thick were collected from trees from
134 different forests compartments in the Sinop micro-region. These samples were obtained
135 from the base of the first commercial log, approximately 1 m above the ground level, or
136 immediately above the sapopemas. We collected 9 discs samples from *A. leiocarpa*, 10
137 from *E. uncinatum*, 13 from *H. excelsum*, and 11 from *T. burserifolia*. The samples were
138 dried and polished and the growth rings were measured with an accuracy of 0.01 mm on
139 a LINTAB measurement table (Frank Rinn, Heidelberg, Germany), using the TSAP-
140 Win software (Rinn, 1996). Crossdating was carried out among radii of each tree and
141 among trees.

142 The mean increment and passage time were analyzed by dbh class. We adjusted the
143 growth models of Gompertz, Johnson-Schumacher, Lundqvist-Korf, Logistic,
144 Monomolecular, and Schumacher for each species (Burkhart; Tomé, 2012).

145 The values of the asymptotes (β_0) were fixed at the upper limit of the largest diametric
146 class recorded in the 100% inventories used. To increase modeling accuracy, we used
147 the non-parametric Bootstrap method with 100 interactions (Miller, 2004), previously
148 used in studies of modeling growth in diameter (Brienen, 2005; Mattos et al., 2015;
149 Canetti et al., 2017). The models were fitted by non-linear regression using the PROC
150 NLMIXED procedure in the SAS® software. The most suitable growth model by

151 species was selected based on the relative residual standard error ($S_{yx\%}$), corrected
152 Akaike and Bayesian information criteria.

153 **Obtaining growth curves in individual volume for each species**

154 Initially, the commercial height at each diameter was obtained to estimate the
155 commercial volume at each age and to relate it to the diametric growth curve. The
156 commercial height/dbh ratio of 30 trees (randomly selected) per species was fitted by
157 non-linear regression (PROC NLMIXED procedure in the SAS® software) according to
158 equation 1 (Schöngart, 2008). Of the 30 trees, four came from sampling inventories (20
159 ≤ dbh < 40 cm) and 26 from 100% inventories (dbh ≥ 40 cm). This selection method
160 was adopted due to the difference of inclusion levels among inventories and the varying
161 sizes of the measured areas.

162 To calculate the wood volume, we used commercial height and dbh for each age
163 (obtained from the diametric growth equation), and taper functions developed for the
164 municipality of Santa Carmem (MT) to calculate the wood volume. For *E. uncinatum*
165 and *T. burserifolia*, we used species-level taper functions (equations 2 and 3,
166 respectively) developed by Lanssanova (2012). For *A. leiocarpa* and *H. excelsum* we
167 used the general taper function for the municipality (equation 4) developed by
168 Lanssanova et al. (2018).

169 The d_i/dbh ratio of the growth samples was applied to calculate the youngest diameters
170 at the dbh, from which the volume at each age was calculated. As a result, the volume
171 growth curve of the individual tree was obtained for each species. From the volume
172 growth curves, the mean annual volume increment (MAI_v) and current annual volume
173 increment (CAI_v) curves for individual trees were obtained according to equations 5 and
174 6.

$$H = \frac{dbh\beta_0}{dbh + \beta_1} \quad (1)$$

$$\frac{d_i}{dbh_{E.uncinatum}} = 1.20 + 2.97\frac{h_i}{H} + 10.95\left(\frac{h_i}{H}\right)^2 + 21.15\left(\frac{h_i}{H}\right)^3 + 19.51\left(\frac{h_i}{H}\right)^4 + 6.80\left(\frac{h_i}{H}\right)^5 \quad (2)$$

$$\frac{d_i}{dbh_{T.burserifolia}} = 1.13 + 1.89\frac{h_i}{H} + 7.16\left(\frac{h_i}{H}\right)^2 + 14.02\left(\frac{h_i}{H}\right)^3 + 12.56\left(\frac{h_i}{H}\right)^4 + 4.15\left(\frac{h_i}{H}\right)^5 \quad (3)$$

$$\frac{d_i}{dbh_{General}} = 1.21 + 2.94\frac{h_i}{H} + 10.94\left(\frac{h_i}{H}\right)^2 + 20.46\left(\frac{h_i}{H}\right)^3 + 17.93\left(\frac{h_i}{H}\right)^4 + 5.90\left(\frac{h_i}{H}\right)^5 \quad (4)$$

$$MAI_v = \frac{v_t}{t} \quad (5)$$

$$CAI_v = v_{t+1} - v_t \quad (6)$$

where: dbh = diameter at 1.30 m above ground level (cm); d_i = diameter at the sample collection height (disc sample, cm); h_i = height of sample collection (m); H = commercial height of the tree (m); β_0 and β_1 = model parameters fitted by non-linear regression; MAI_v = mean annual volume increment (m^3); CAI_v = current annual volume increment (m^3); v_t = accumulated commercial volume (m^3), at different ages; t = age (years), according to the diametric growth curve.

The age of biological rotation of individual tree was obtained at the intersection point of the CAI_v and MAI_v curves. If the age of biological rotation was not reached with the ages of the available samples, we extrapolated the growth equation in diameter to estimate that age. For the extrapolated diameters, the commercial volume and CAI_v and MAI_v were calculated, following the same procedures.

Obtaining growth curves in volume of the population of each species

To obtain growth in volume per unit area for the population of each species over time, individual growth curves in volume were associated with the PDFs. It was assumed that a species diametric distribution follows the same pattern that occurred in the past (Gotelli, 2008; Lundqvist, 2017). From this premise, the maximization of the population volume increments was obtained. The population was defined hereby as the number of trees from the first to the last diametric class in which there were individuals alive until the moment "t".

The input of the PDFs is the dbh of the trees and the output is the estimated number of trees per unit area. The growth equations developed to generate the diameter values were used to estimate the number of trees alive at each time "t", considering the species' growth curve. The procedure illustrated in Fig. 1 allowed us to estimate the population's diametric evolution over time (time x number of trees ha^{-1}). As the actual diametric distributions were established with data from dbh ≥ 20 cm, the calculations were performed from that diameter, according to the following procedure:

I. The number of trees at each time "t" (identified by the PDF) was multiplied by the volume of the individual tree (v) at each time, resulting in the population production curve (V) at each time referring to the species growth curve;

II. From the population volume production curve, MAI_v and CAI_v were derived (equations 5 and 6).

Obtained from:

Pdf	Dbh growth equation		Taper equations	N x v		Derivatives of V
N (trees ha^{-1})	**Time (years)**	**Dbh (cm)**	**v (m^3)**	**V (m^3 ha^{-1})**	**MAIv (m^3 ha^{-1} $year^{-1}$)**	**CAIv (m^3 ha^{-1} $year^{-1}$)**
0.0955	70	27.8696	0.3783	0.0361	5.16×10^{-4}	1.86×10^{-3}
0.0957	71	28.4297	0.3971	0.0380	5.35×10^{-4}	1.88×10^{-3}
0.0958	72	28.9951	0.4166	0.0399	5.54×10^{-4}	1.91×10^{-3}
0.0958	73	29.5656	0.4368	0.0419	5.73×10^{-4}	1.93×10^{-3}
0.0957	74	30.1413	0.4577	0.0438	5.92×10^{-4}	1.95×10^{-3}
0.0955	75	30.7221	0.4793	0.0458	6.10×10^{-4}	1.97×10^{-3}

Fig. 1. Scheme showing the methodological process for obtaining the curves of volume increment of the population. The boxes with red outline inform the data source of the column to which the arrows are directed. PDFs = probability density functions; N = number of trees per hectare; dbh = diameter at 1.30 m above ground level; v = volume of individual tree; V = species population volume (m^3 ha^{-1}); MAI_v = mean annual volume increment; and CAI_v = current annual volume increment.

Management simulations

The projection method by diametric class (Alder, 1995) was used to compare the volumetric increments obtained from the different combinations of cutting cycle and minimum cutting diameter (MCD), according to the following management scenarios:

I. MCD = 50 cm and cutting cycle = 35 years, according to current legislation (Brasil, 2006);

II. MCD defined by the biological rotation age of the population (intersection of the MAI_v and CAI_v curves) and cutting cycle = 35 years;

III. MCD defined by the maximum CAI_v and biological rotation age of the population and cutting cycle calculated using equation 7 (Schöngart, 2008).

$$Cutting\ cycle(years) = \frac{Age_{Max.CAIv}}{0.1 dbh_{Max.CAIv}} \quad (7)$$

where Cutting cycle (years) = time interval between explorations in the forest (Schöngart, 2008); $dbh_{Max.CAIv}$ = minimum cutting diameter, defined as the diameter at which the species reaches the maximum CAI_v; $Age_{Max.CAIv}$ = age at which the species reaches the MCD.

IV. MCD defined by dbh in which the maximum CAIv occurs at the individual tree level and cutting cycle calculated according to Schöngart (2008);

V. MCD defined by the dbh of biological rotation age of the population in volume and increasing cutting cycles (10 to 70 years).

The mathematical procedure for simulations in the projection method by diametric class is presented in equation 8 (Alder, 1995).

$$N_{k,t+1} = N_{k,t} + I_k - O_k - M_k - H_k \quad (8)$$

where $N_{k,t+1}$ = number of trees in dbh class *k* in period *t+1*; $N_{k,t}$ = number of trees in class *k* in period *t*; I_k = ingrowth in class *k* during the period; O_k = number of trees passing from class *k* to subsequent classes, M_k = mortality in class *k*; H_k = trees logged during the period.

The matrices were built from the 30-cm dbh class, for every 5 years (t), until reaching the desired cutting cycle. We considered the wood volume of trees with a dbh higher than the MCD the volume to be harvested (H_k). The following data were used:

I. Initial diametric structure ($N_{k,t}$): obtained from PDFs fitted by species, considering dbh ≥ 30 cm;

II. Mean increment by diameter class (obtained from the growth equations). The number of trees passing to the subsequent classes (O_k) was calculated from the passage time between diametric classes (equation 9), as described by Alder (1995).

$$O_k = \frac{t.i}{w} \quad (9)$$

where: O_k = number of trees migrating from class *k* to subsequent classes during the period considered; i = mean increment (cm year^{-1}) of the diametric class *k* (obtained from the growth series); w = interval between diametric classes (10 cm in the present study); t = period considered.

III. Ingrowth (I_k): the number of trees in the 20-cm diameter class (smallest dbh class obtained) was considered as ingrowth.

IV. Mortality (M_i): the mortality was estimated using equation 10 adapted from Lundqvist (2017).

$$M_i = 100\left(1 - \frac{N_{i+1} i_{i+1}^{\frac{2}{t_i + t_{i+1}}}}{N_i i_i}\right) \quad (10)$$

where: M_i = percentage of annual mortality in diametric class *i*; N_i = number of trees in class *i*; N_{i+1} = number of trees in the class subsequent to *i*; i_i and i_{i+1} = mean annual increment in diameter (cm) of classes *i* and *i+1* (obtained from the growth equation); t_i and t_{i+1} = passage time (years) from the diametric classes *i* and *i+1* to the subsequent classes (obtained from the growth equation).

After obtaining the final diametric structure of the projection matrix by diametric class, the number of trees was converted into volume (applying the taper functions previously described) to obtain the total wood production in the considered period. This production was divided by the cutting cycles, in order to proportionally compare the production of the tested MCD and cutting cycles.

Results

Diametric structure

When testing the adherence of general probability density functions (PDFs) adjusted to the measured density distributions for each species and for each forest compartment, the majority of tested PDF fitted (Table 1). The only exceptions found were the Normal function (all areas) and the Beta function (areas 3, 4 and 6) for *T. burserifolia.*

Table 1. Goodness-of-fit test of the probability density function (PDF) fitted considering the total data set to the observed diametric distributions in each study area by the Kolmogorov-Smirnov test.

Species	D	PDF	Area 1	Area 2	Area 3	Area 4	Area 5	Area 6
Apuleia leiocarpa	$D_{calc.}$	Normal	0.048	0.100	0.078	0.139	0.089	0.063
		Beta	0.047	0.094	0.081	0.141	0.092	0.062
		Gamma	0.054	0.100	0.070	0.154	0.077	0.054
		Log Normal	0.075	0.109	0.080	0.167	0.060	0.048
		Johnson's SB	0.045	0.095	0.075	0.147	0.085	0.060
		Weibull 3p	0.044	0.095	0.076	0.145	0.087	0.061
		$D_{tab.}$	0.410	0.410	0.521	0.565	0.432	0.375
Erisma uncinatum	$D_{calc.}$	Normal	0.049	0.256	0.084	0.055	0.082	0.044
		Beta	0.072	0.190	0.151	0.107	0.026	0.050
		Gamma	0.069	0.261	0.081	0.045	0.099	0.060
		Log Normal	0.095	0.278	0.063	0.068	0.122	0.085

		Johnson's SB	0.047	0.257	0.083	0.056	0.082	0.043
		Weibull 3p	0.049	0.253	0.088	0.061	0.078	0.038
		$D_{tab.}$	0.189	0.294	0.240	0.240	0.270	0.270
Hymenolobium excelsum	$D_{calc.}$	Normal	0.124	0.124	0.124	0.124	0.151	0.124
		Beta	0.061	0.060	0.060	0.060	0.131	0.092
		Gamma	0.049	0.061	0.062	0.056	0.132	0.093
		Log Normal	0.051	0.068	0.065	0.068	0.132	0.093
		Johnson's SB	0.049	0.058	0.063	0.050	0.129	0.090
		Weibull 3p	0.038	0.051	0.067	0.054	0.125	0.086
		$D_{tab.}$	0.565	0.624	0.521	0.521	0.708	0.708
Trattinnickia burserifolia	$D_{calc.}$	Normal	0.238*	0.238*	0.238*	0.238*	0.238*	0.238*
		Beta	0.187	0.170	0.170*	0.170*	0.170	0.170*
		Gamma	0.180	0.149	0.149	0.149	0.149	0.149
		Log Normal	0.167	0.119	0.106	0.106	0.106	0.106
		Johnson's SB	0.127	0.071	0.071	0.071	0.071	0.092
		Weibull 3p	0.149	0.080	0.046	0.042	0.054	0.077
		$D_{tab.}$	0.193	0.183	0.166	0.170	0.178	0.169

Area = sampled forest compartment; Dcalc. = maximum absolute value between fitted PDF and observed values in each compartment; Dtab. = critical value of Kolmogorov-Smirnov test ($\alpha = 0,05$); * = the PDF did not fit to the observed values (Dtab. $\leq$ Dcalc.).

When considering the adherence of all PDFs tested to the total set of observed data by species all functions fitted. The Gamma function fitted better to the observed data for *A. leiocarpa*, the Normal function for *E. uncinatum* and *H. excelsum,* and the Weibull with three parameters for *T. burserifolia* (Fig. 2). A unimodal pattern was observed for the diametric distributions of *A. leiocarp*a, *E. uncinatum*, and *H. excelsum*. On the other hand, *T. burserifolia* decreased in a regular number of trees, similar to the negative

286 exponential distribution. The decreased tendency starts in *H. excelsum* at 45-cm, in *A.*

287 *leiocarpa* at 55-cm, and in *E. uncinatum* at 75-cm diameter.

288

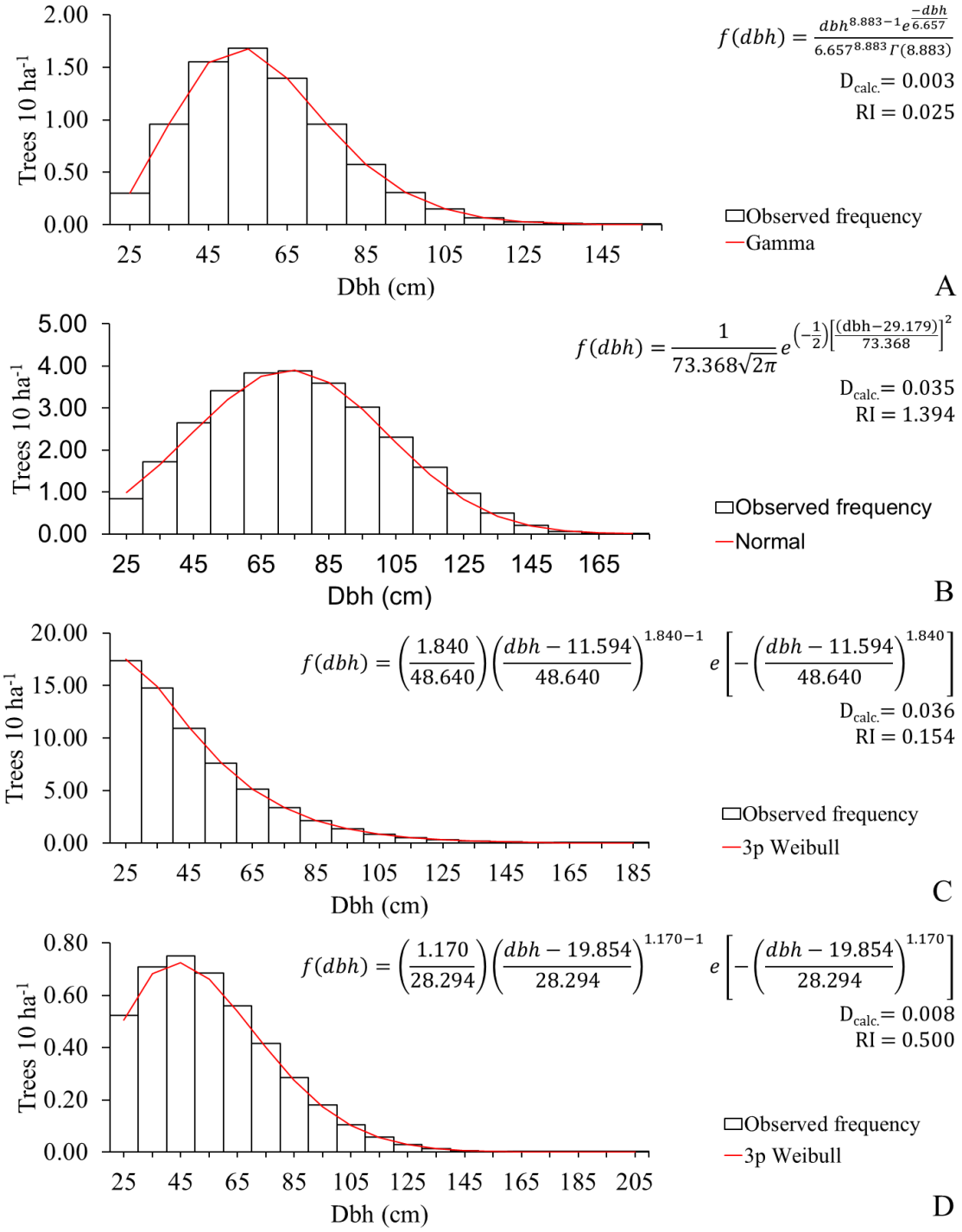

289

290 Fig. 2. Probability density functions with better fitting for *Apuleia leiocarpa* (A), *Erisma uncinatum* (B),

291 *Hymenolobium excelsum* (C) and *Trattinnickia burserifolia* (D). Dbh = diameter at 1.30 m above ground

level (cm); Γ = gamma function; Dcalc. = maximum absolute value between fitted pdf and observed values in each compartment; IR = error index (Reynolds et al., 1988).

Height/dbh ratio

The fitted height/dbh model showed satisfactory statistics and residual distribution for all species (Fig. 3). The species that reached the highest commercial heights were *E. uncinatum* and *H. excelsum*. The largest commercial height range occurred before reaching 60-cm dbh, ranging from 6.5 to 10.9 m. After 60-cm dbh, the commercial heights tended to stabilize, ranging from 10.9 to 13.4 m.

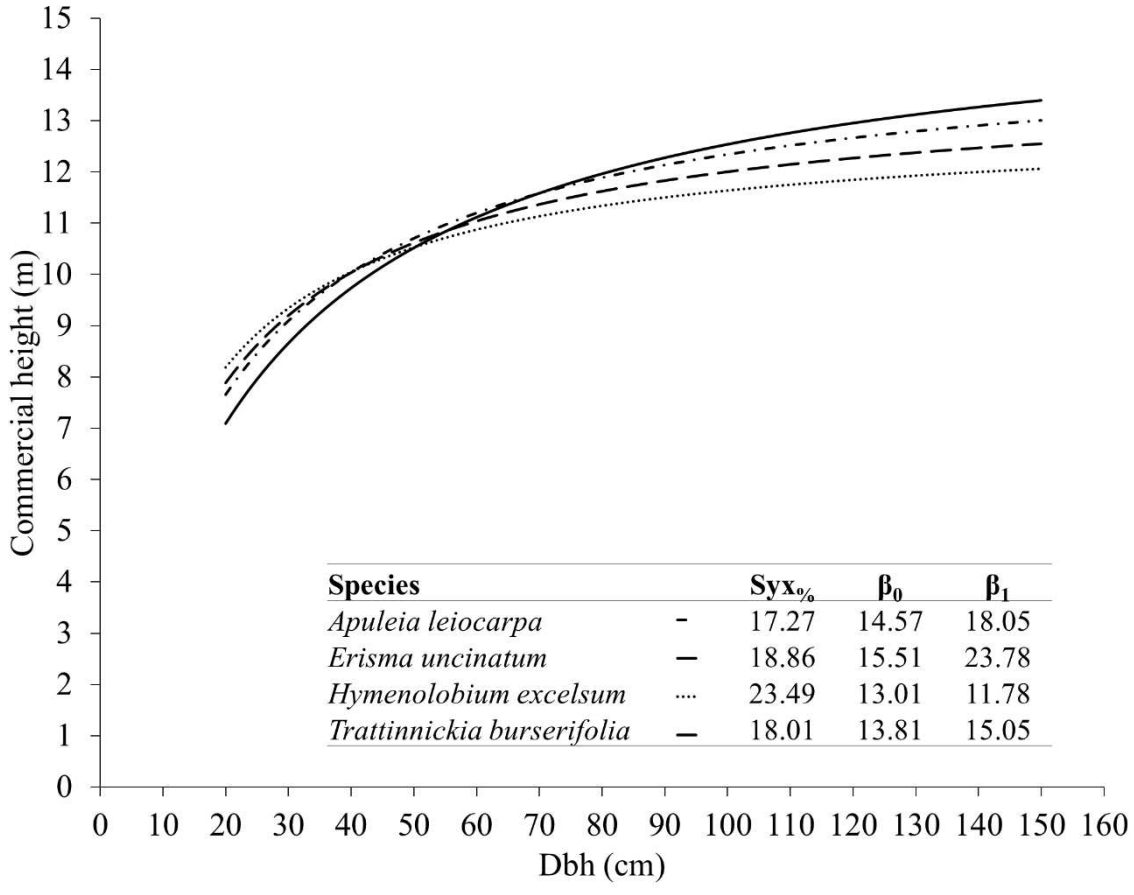

Fig. 3. Heigh/dbh models of *Apuleia leiocarpa*, *Erisma uncinatum*, *Hymenolobium excelsum*, and *Trattinnickia burserifolia*. dbh = diameter at 1.30 m above ground level (cm); β_0 and β_1 = equation parameters fitted by non-linear regression; $S_{yx\%}$ = relative residual standard error (%)

306

307 **Diametric increment in dbh classes**

308 The mean increment by dbh class and passage time are shown in Fig. 4 and 5. *Apuleia*
309 *leiocarpa* presented an initial increase in dbh increment, and a decrease for the upper
310 diameter classes (Fig. 4A), characterizing the U shape for the passage time (Fig. 5A).
311 *Erisma uncinatum*, *H. excelsum*, and *T. burserifolia* showed a higher increase in the
312 upper classes (Fig. 4 B, C and D), assuming a decreasing passage time (Fig. 5 B, C and
313 D).

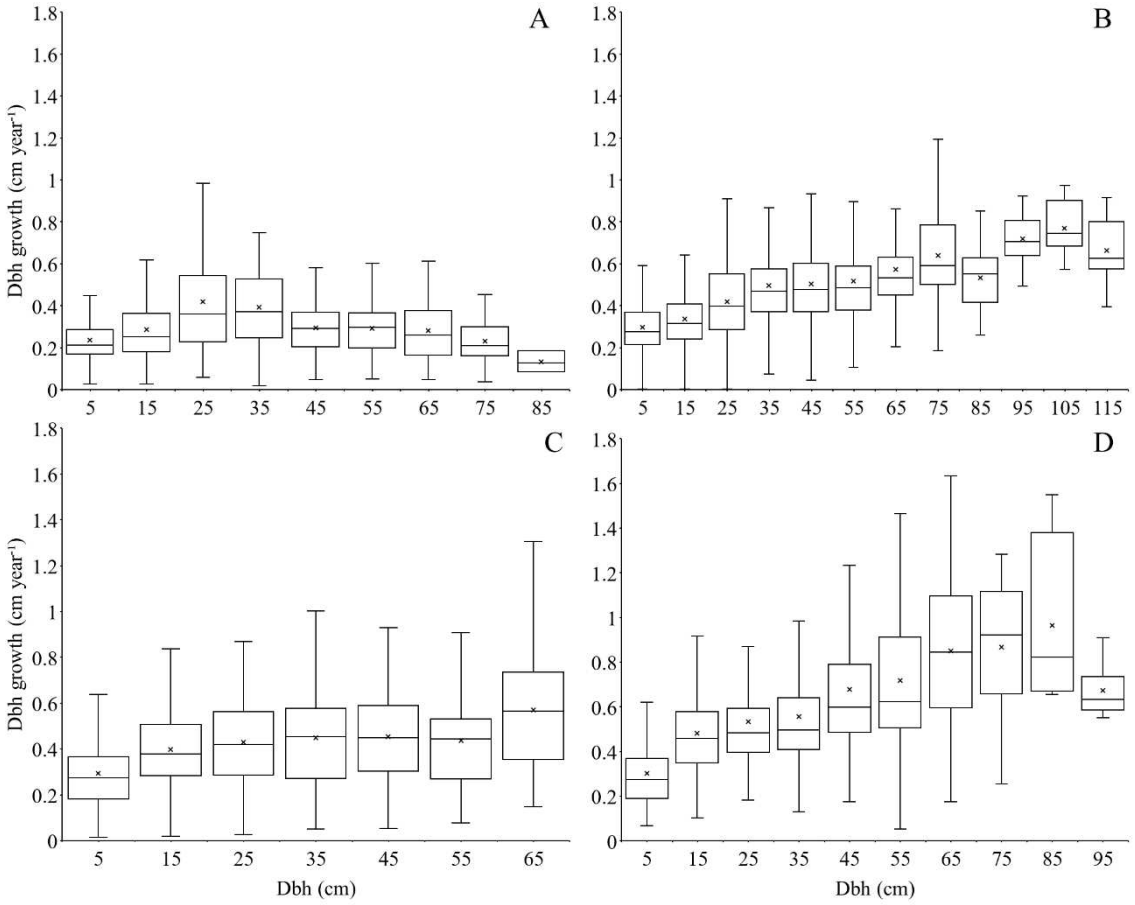

314

315 Fig. 4. Boxplot of the mean annual periodic increment by diameter class of *Apuleia leiocarpa* (A), *Erisma*
316 *uncinatum* (B), *Hymenolobium excelsum* (C), and *Trattinnickia burserifolia* (D). Markers (x) represent the
317 mean increment per diameter class, which were calculated only for the diameter classes with three or
318 more trees. Dbh = diameter at 1.30 m above ground level.

319

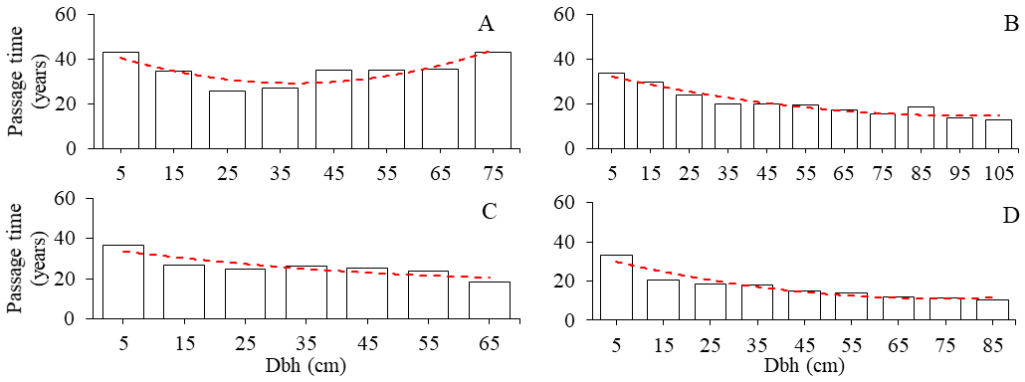

Fig. 5. Mean passage time by diameter class for *Apuleia leiocarpa* (A), *Erisma uncinatum* (B), *Hymenolobium excelsum* (C), and *Trattinnickia burserifolia* (D) and their respective tendency lines. Only passage times for diameter classes with three or more trees were considered. Dbh = diameter at 1.30 m above ground level.

Modeling accumulated diameter growth and generating increment curves

The Johnson-Schumacher model better fitted the time series of *A. leiocarpa* and *H. excelsum*, while the Gompertz was better for *E. uncinatum* and *T. burserifolia*. For diameter growth, *A. leiocarpa* and *H. excelsum* reached the point of maximum tangency close to 35 cm and 50 cm, respectively, registering lower increments after these diameter classes (Fig. 6 A and C). However, *E. uncinatum* and *T. burserifolia* did not reach this point within the measured diameters (Fig. 6 B and D), showing upward growth throughout the entire time series.

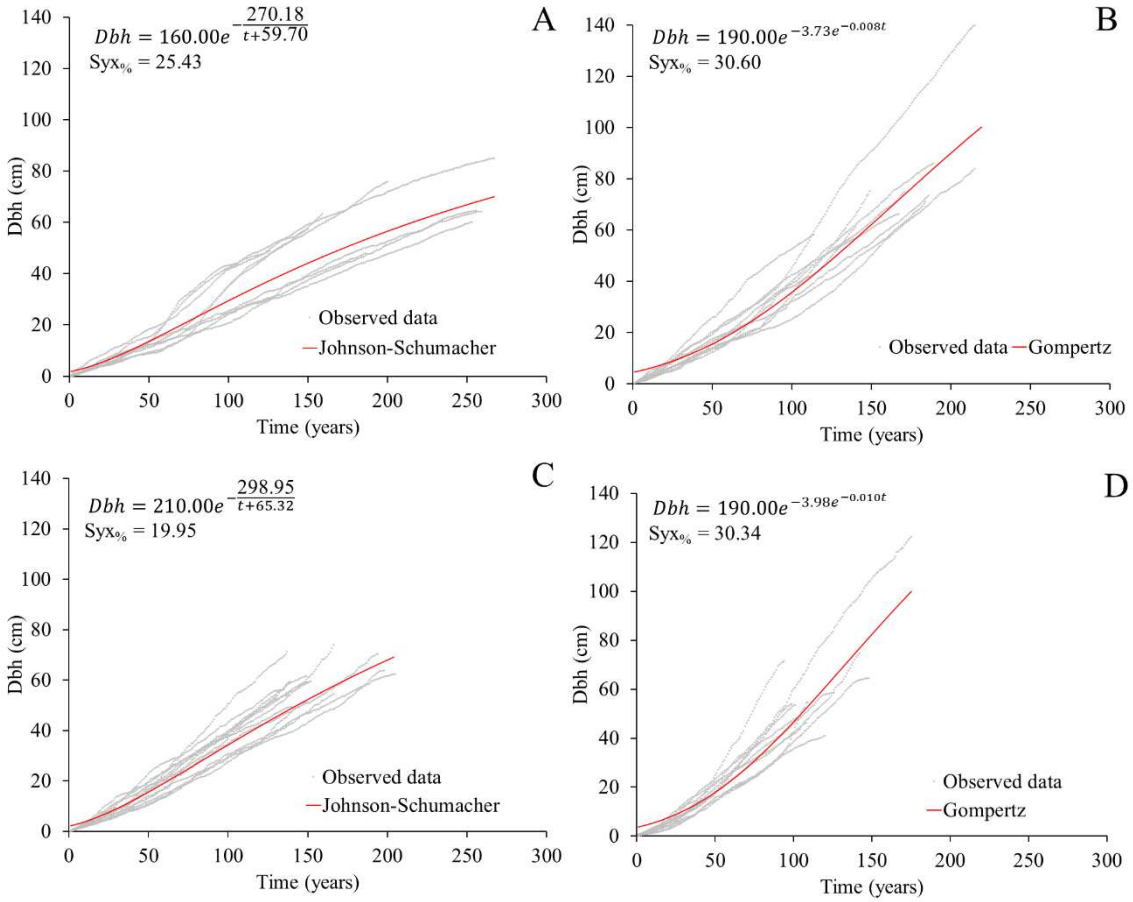

Fig. 6. Accumulated diametric growth equations fitted for *Apuleia leiocarpa* (A), *Erisma uncinatum* (B), *Hymenolobium excelsum* (C), and *Trattinnickia burserifolia* (D). The growth equations were fitted for the ages represented by three or more samples. Dbh = diameter at 1.30 m above ground level; t = time (years); $S_{yx\%}$ = Relative Residual Standard Error (%).

Apuleia leiocarpa, *E. uncinatum***,** and *T. burserifolia* reached the maximum current annual increment in volume (CAI_v) when considering the available data (Fig. 7 A, B and D). The maximum CAI_v for *H. excelsum* was estimated at approximately 245 years (Fig. 7C).

For the four species, the growth equation was used to estimate the biological rotation age, which for individual trees occurred at the 95-cm dbh for A. *leiocarpa*, 121-cm for *H. excelsum*, and 165-cm for *E. uncinatum* and *T. burserifolia*. The maximum CAI_v

348 occurred close to the 60-cm dbh for *A. leiocarpa*, 80-cm for *H. excelsum*, and 120-cm
349 for *E. uncinatum* and *T. burserifolia* (Table 2).

350

351 Table 2. Estimated ages and diameters on the biological rotation and the maximum current annual
352 increment of individual tree volume for the species.

Species	Biological rotation		Maximum CAI_v	
	Dbh (cm)	Age (years)	Dbh (cm)	Age (years)
Apuleia leiocarpa	95	455	63	231
Erisma uncinatum	165	409	119	257
Hymenolobium excelsum	121	480	80	245
Trattinnickia burserifolia	165	319	118	203

353 Dbh = diameter at 1.30 m above ground level; maximum CAI_v = maximum current annual increment for
354 individual tree volume; Biological rotation = intersection of the CAI_v and MAI_v (current and mean annual
355 increment for individual tree volume) curves.

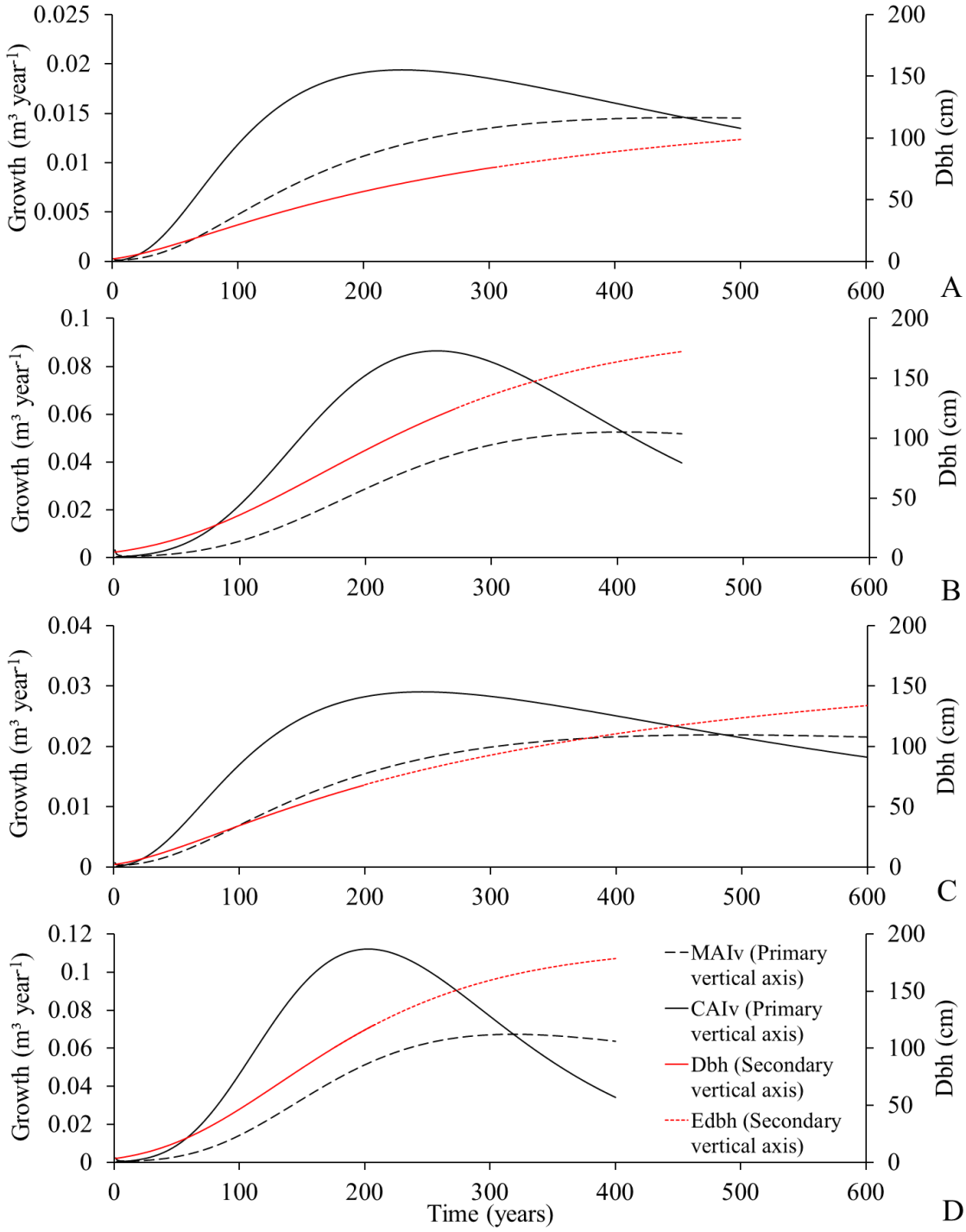

Fig. 7. Volumetric increment curves (black) and dbh growth equation (red) for *Apuleia leiocarpa* (A), *Erisma uncinatum* (B*), Hymenolobium excelsum* (C), and *Trattinnickia burserifolia* (D). In the primary y-axis: MAI_v = mean annual volumetric increment; CAI_v = current annual volumetric increment. On the secondary y-axis: dbh = diameter at 1.30 m above ground level (cm) (growth equation fitted within the measured data range); Edbh = accumulated diameter at 1.30 m above ground level (growth equation outside the measured data range).

363 **Growth by species population**

364 The maximum CAI_v and biological rotation ages of the population volume (Table 3;
365 Fig. 8) occurred in lower diameters than those recorded for individual trees (Fig. 7;
366 Table 2). Those ages were reached for diameters within the stem samples. There was
367 therefore no need for the extrapolation of the volume growth equations that was
368 required for the individual diameter growth (Fig. 7).

369

370 Table 3. Estimated ages and diameters on the biological rotation and the maximum current annual
371 increment by species population.

Species	Biological rotation		Max. CAI_v	
	Dbh (cm)	Age (years)	Dbh (cm)	Age (years)
Apuleia leiocarpa	58	203	44	160
Erisma uncinatum	86	192	64	154
Hymenolobium excelsum	52	150	37	106
Trattinnickia burserifolia	58	116	34	80

372 Dbh = diameter at 1.30 m above ground level; Max. CAI_v = maximum current annual increment for
373 population volume; biological rotation = intersection of the curves of CAI_v and mean annual increment in
374 volume for individual tree.

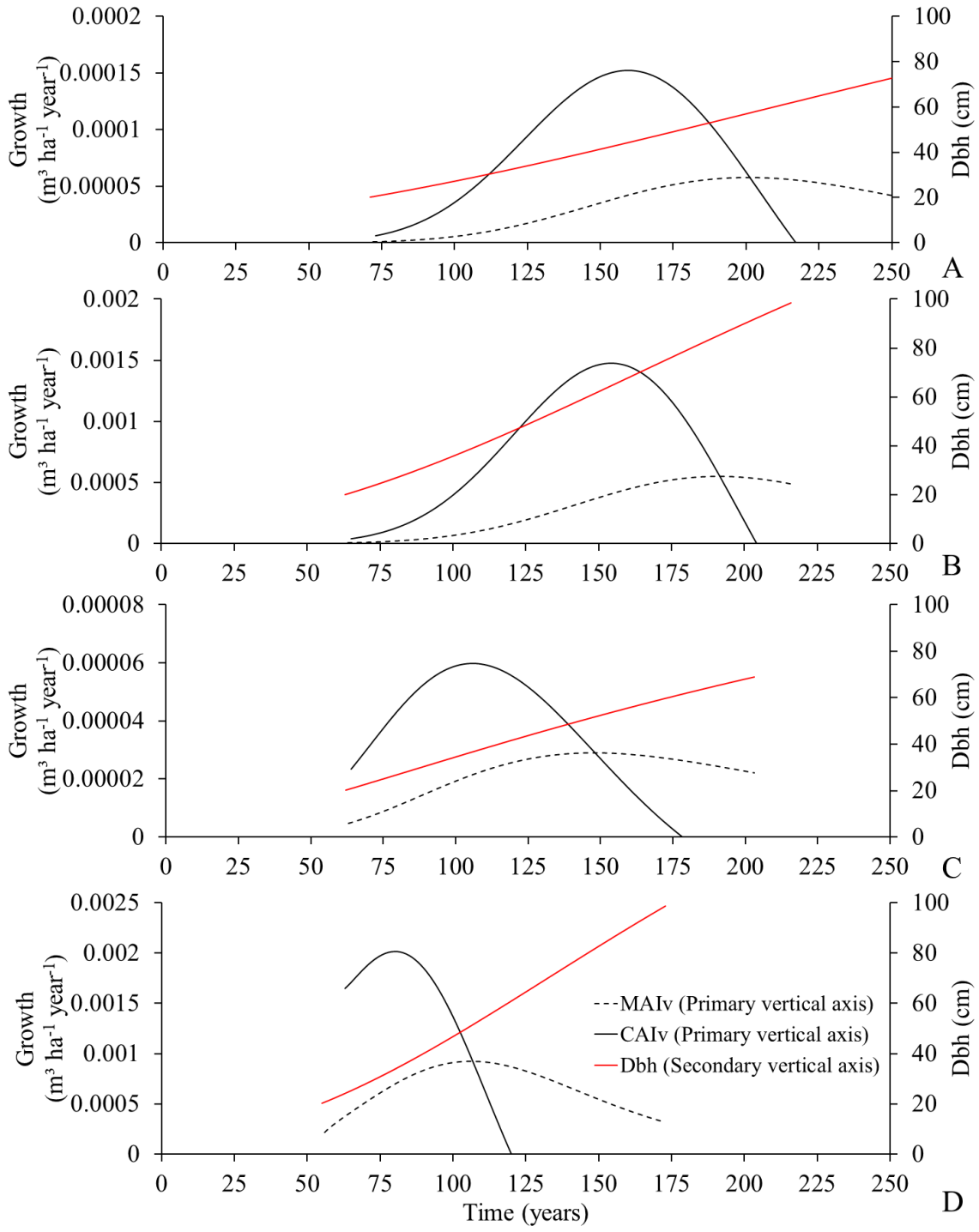

375

376 Fig. 8. Volumetric and diametric increment curves for the population of *Apuleia leiocarpa* (A), *Erisma*
377 *uncinatum* (B), *Hymenolobium excelsum* (C) and *Trattinnickia burserifolia* (D) (dbh ≥ 20 cm). In the
378 primary y-axis: MAI_v = mean annual increment in volume; CAI_v = current annual increment in volume.
379 In the secondary y-axis: dbh = diameter at 1.30 m above ground level (cm), obtained from the growth
380 equation.

381

382 **Minimum cutting diameter (MCD) and cutting cycle simulations**

383 The MCD criteria determined by the biological rotation age of the population and with
384 short cutting cycles (10 years) (Table 4) resulted in a higher annual volume yield for the
385 four species. For *A. leiocarpa*, *H. excelsum* and *T. burserifolia*, the maximum CAI_v age
386 of the population and the cutting cycle, as suggested by Schöngart (2008), resulted in
387 the least increment (m^3 ha^{-1} $year^{-1}$) of all criteria. For *E. uncinatum* the management
388 criteria defined in the legislation resulted in the least increment.

389

390 Table 4. Simulation results using different criteria for defining the minimum cutting diameter and cutting
391 cycle.

Species	MCD	Law	Rot. $_{pop.}$	Rot. $_{pop.}$	$CAI_{v\ pop.}$	$CAI_{v\ ind.}$	Rot. $_{pop.}$	Rot. $_{pop.}$
	Cutting cycle	Law	Law	SM	SM	SM	Short	Long
Apuleia leiocarpa	MCD (cm)	50	57	57	44	63	57	57
	Cycle (years)	35	35	37	37	37	10	70
	Inc. (m^3 ha^{-1} $year^{-1}$)	0.0078	0.0107	0.0106	0.0055	0.0113	**0.0159**	0.0086
	Vol. (m^3 100 ha^{-1})	27.46	37.52	39.09	20.49	41.82	15.86	60.53
Erisma uncinatum	MCD (cm)	50	86	86	64	119	86	86
	Cycle (years)	35	35	22	22	22	10	70
	Inc. (m^3 ha^{-1} $year^{-1}$)	0.0238	0.1140	0.1238	0.0643	0.0800	**0.1427**	0.0795
	Vol. (m^3 100 ha^{-1})	83.27	398.90	272.28	141.51	176.01	142.74	556.66
Hymenolobium excelsum	MCD (cm)	50	52	52	37	80	52	52
	Cycle (years)	35	35	31	31	31	10	70
	Inc. (m^3 ha^{-1} $year^{-1}$)	0.0051	0.0054	0.0055	0.0029	0.0049	**0.0069**	0.0046

	Vol. (m^3 100 ha^{-1})	17.69	18.84	17.03	8.86	15.31	6.90	31.86
Trattinnickia burserifolia	MCD (cm)	50	58	58	34	118	58	58
	Cycle (years)	35	35	17	17	17	10	70
	Inc. (m^3 ha^{-1} $year^{-1}$)	0.1511	0.2027	0.2776	0.1216	0.1966	**0.3622**	0.1384
	Vol. (m^3 100 ha^{-1})	528.95	709.37	471.85	206.64	334.20	362.25	968.89

MCD = minimum cutting diameter; Cycle = cutting cycle; SM = Schöngart (2008) method; $Rot._{pop.}$ = biological rotation age of the population; $CAI_{v\ pop.}$ = maximum current annual increment of the population; Legisl. = Normative Instruction parameters (Brasil, 2006); Inc. = simulated mean annual volumetric increment; Vol. (m^3 100 ha^{-1}) = total volume produced in a 100-ha area, during the cutting cycle length. The highest simulated annual increments in volume are presented in bold.

Considering the MCD defined by the population's biological rotation age, the annual volumetric production decreased for the four species as the cutting cycle increased (Fig. 9).

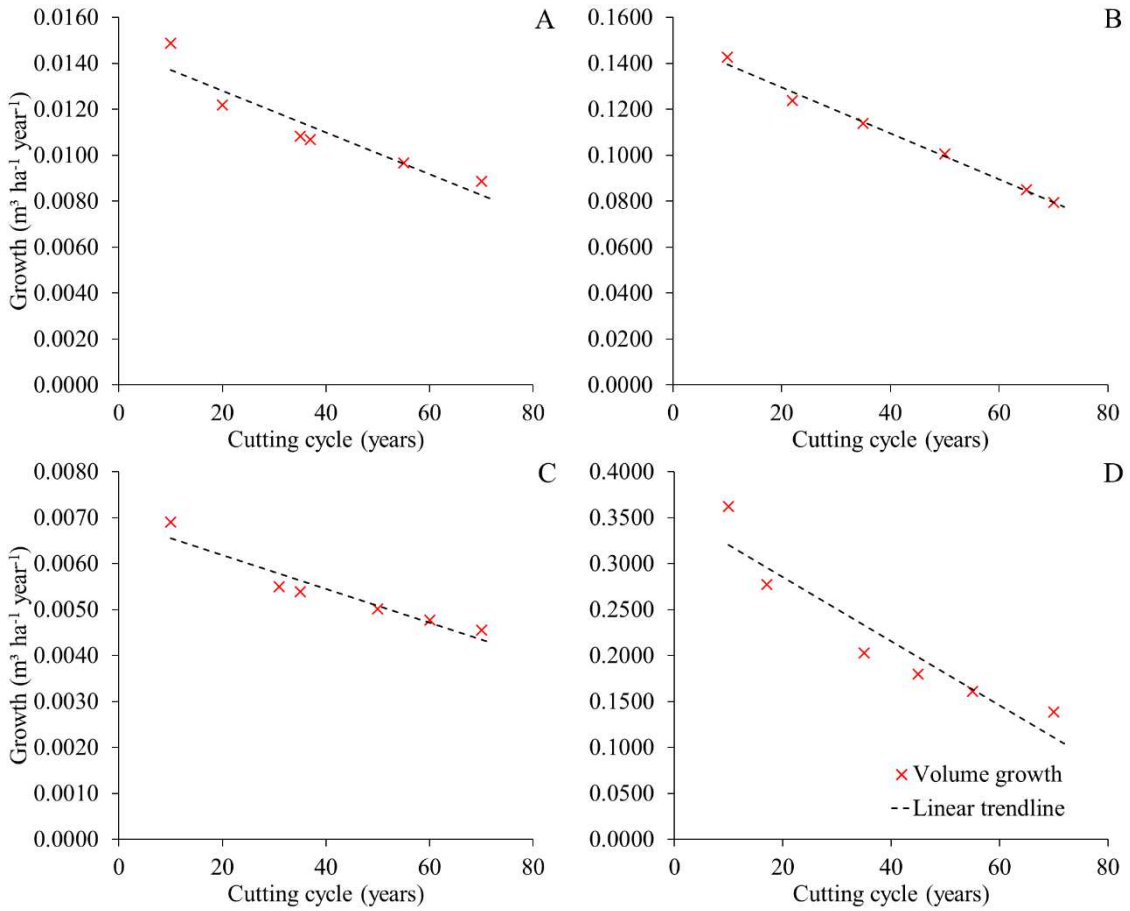

Fig. 9. Annual volume increment by the MCD defined by the population's biological rotation age and different cutting cycles for *Apuleia leiocarpa* (A), *Erisma uncinatum* (B), *Hymenolobium excelsum* (C), and *Trattinnickia burserifolia* (D).

Discussion

Diametric distribution pattern of the species

Most of the probability density functions (PDFs) (Table 1) fitted to data in each forest compartment. Thus, a single PDF per species was fitted at the Sinop microregion (Fig. 2). Fitting only one PDF per species across the microregion suggests the existence of similarities in the species diametric structure in the typology, contrasting to the claim that ecosystems are chaotic and disordered (O'Hara, 2014). According to this same author, ecosystems are not deterministic or ordered, due to the occurrence of repeated disturbances on small scales, which prevent the forest from being homogeneous over

415 time. However, for Larson (1992), the occurrence of environmental or anthropic
416 disturbances combined with the genetic variation of mixed forest does not imply that
417 forest development patterns cannot be discerned.
418 Also, the micro-region's pattern agrees with the demographic equilibrium theory, which
419 states that the diameter distribution balance may be scalar (Muller-Landau et al., 2006).
420 The forest structure is regulated by general principles of growth, mortality (Wang et al.,
421 2009) and ecological succession (Oliver, 1992).
422 Even in distant or geographically isolated regions, species with resembling
423 physiological and morphological characteristics can have a similar population structure
424 (Oliver, 1992). This occurs because the structures repeat over time in the forest (Gotelli,
425 2008). Diametric structure models allow us to infer the diameter in which tree number
426 reduces as a result of stagnant growth and increased mortality (Durrieu de Madron;
427 Forni, 1997; Braz et al., 2014).
428 Ecologists use the diametric structure to indicate the health of the forest. A high number
429 of smaller trees, as recorded for *T. burserifolia* (Fig. 2D), would represent forest
430 sustainability, since it would restore the upper classes (Kohyama, 1986; Muller-Landau
431 et al., 2006; Wang et al., 2009). These considerations originated from De Liocourt's
432 (1898) and Meyer's (1952) theories that state the concept of a balanced forest following
433 a negative exponential pattern.
434 However, several studies have found that some forest types and many individual species
435 may not follow such a negative exponential model (Condit et al., 1998; Dawkins;
436 Philip, 1998; Nyland, 2002; Pascal, 2003; Braz, 2010; Braz et al., 2014; Hossain et al.,
437 2015), as occurred for three of the species in this study (Fig. 2 A, B and C).
438 A minor number of smaller trees, as recorded for *A. leiocarpa*, *E. uncinatum* and *H.*
439 *excelsum*, could indicate that the populations are declining (Condit, 1998; Hossain et al.,

2015). However, the forest diametric structure is not the only indicator defining population maintenance. Schaaf et al. (2006) pointed out that the highest density does not guarantee the species maintenance in the community, but their ability to compete within the ecological niche does. The authors stated that if the species has few trees with smaller diameters, but if the individuals tolerate competition for light in the lower canopy, they can remain in the forest. Therefore, it is necessary to consider other factors, particularly the species growth in the diameter classes (Condit et al., 1998).

Braz et al. (2014) identified over 60% of the basal area in the upper stratum in the Sinop micro-region, a situation described by Pascal (2003). This author stated that the deficit of trees in some dbh classes or the accumulation in larger dbh classes can result from different causes. For example, a massive fruiting and germination due to favorable climatic conditions can engender an overstock of trees in a particular dbh class. These individuals can outgrow to larger dbh classes after a certain time, resulting in an imbalanced diametric structure curve. These same individuals may be stagnated in a certain dbh class when under the closed canopy of the forest.

An over-stocked upper stratum may have its regeneration constrained due to inadequate access to light by trees in the lower canopy (Yegang; Jinxuan, 1988; Lamprecht, 1990; Felfili, 1997; Nyland, 2002; Bettinger et al. 2009). In such cases, some species may need a longer time scale to regenerate (Felfili, 1997). Over time, this factor de-characterizes both the negative exponential structure (Braz, 2010; Bettinger et al., 2009) and the whole forest increment (Dawkins; Philip, 1998).

Production modeling at individual tree level

Commercial height is an essential dendrometric variable for modeling production forests since it is used for volume prediction (Lappi, 1997). Fitting parameters for the commercial height/dbh ratio (Fig. 3) allows us to calculate commercial volumes of

individual trees and stands more accurately where there is no field measuring. Other authors used the commercial height/dbh ratio to model the wood volume in the Amazon Forest (Brienen; Zuidema, 2006a; Fortini; Zarin, 2011; Miranda, Z. P. et al., 2018).

According to Alder (1995), in natural forests the initial growth of trees is slow, followed by a phase of higher increments until it reaches its maximum. After that maximum point, growth reduces until stagnation. *Apuleia leiocarpa*, *E. uncinatum* and *T. burserifolia* followed this pattern (Fig. 4 A, B and D and 5 A, B and D), while *H. excelsum* maintained constant growth during five diameter classes, not exceeding 0.5 cm $year^{-1}$, except in the 65-cm class (Fig. 4C). The constant growth of *H. excelsum* until larger sizes is a feature of late and emerging secondary species (Silva et al., 1985), whose crowns extend above the canopy average level. These functional groups have several micro-habitats during their ontogenesis (Clark; Clark, 1992). They are characterized as partial sciophytes, shade-tolerate in the early development stages. However, they require a high degree of illumination to overcome the intermediate stages to maturity, increasing its growth during canopy opening (Maciel et al., 2017).

The decreasing tendency of passage time (Fig. 5 B, C, and D) for the late secondary species (*E. uncinatum*, *H. excelsum*, and *T. burserifolia*) is also a feature of partial sciophytes, that are shade tolerant, but do not demand shade for growth (Maciel et al., 2017).

The U-shaped passage time of the initial secondary species (*A. leiocarpa*) has already been pointed out by Brienen and Zuidema (2006b) for *Bertholletia excelsa* Bonpl., an initial secondary species (Gouveia et al., 2011). The same tendency was also registered for *Goupia glabra* Aubl. in the micro-region of Sinop-MT (Oliveira et al., 2015), which shows maximum growth in the 25-cm and 35-cm diameter classes, despite being a late secondary species (Araújo et al., 2009), as occurred for *A. leiocarpa* (Fig. 5A).

The biological rotation and maximum CAI_v ages (Fig. 7; Table 2) were consistent with the increment by diameter class (Fig. 4). *Apuleia leiocarpa*, an initial secondary species, reached biological rotation and maximum CAI_v ages in smaller diameters, while *H. excelsum* reached it in intermediate sizes. The other two species achieved biological rotation for an estimated dbh higher than 160 cm. The maximum CAI_v of an individual tree were used in scientific studies to define minimum cutting diameters and cutting cycles for species in Amazonas State (Schöngart, 2008; Rosa et al., 2017; Miranda D. L. C., 2018), and has already been included in State forest law (Amazonas, 2010). If logging happens before the maximum CAI_v or after the maximum MAI_v, the volumetric production will be inefficient. In this case, the species would not have reached or would have passed their optimal growth (Schöngart, 2008; Braz; Mattos, 2015). Therefore, knowing the maximum CAI_v and MAI_v per species is essential for sustainable forest management in the Amazon forest.

The curves of individual wood volume increment indicate the ideal parameters for sustainable management of each species. However, other variables representing the species dynamics must be considered for decision-making. For example, it is essential to define available stock of trees by diameter class and survival rates (Sebben et al., 2008; Free et al., 2014; Groenendijk et al., 2017; Free, 2017).

Volumetric population growth

The maximum CAI_v estimated from the population increment curves occurred for diameters lower than 50 cm for *A. leiocarpa*, *H. excelsum*, and *T. burserifolia*, and at 64-cm diameter for *E. uncinatum* (Table 3; Fig. 8). The dbh when biological rotation age occurs, at which CAI_v and MAI_v curves intersected, was around 50 cm for *A. leiocarpa*, *H. excelsum*, and *T. burserifolia*, while for *E. uncinatum* this occurred at 86 cm. *Erisma uncinatum* has increased growth (Fig. 4) and a high concentration of trees in

515 the upper diameter classes, which explains its yield culmination in larger dbh sizes. This
516 feature suggests the maintenance of larger dbh trees in the forest. In polycyclic
517 management systems, the trees available for logging must reach at least the diameters
518 with the highest growth potential in volume (Miranda, Z. P. et al., 2018) represented by
519 the MCD. For this reason, it is essential to determine the diameter that provides the
520 highest wood production for each species, based on the individual growth and the
521 population demographic characteristics.
522 According to Miranda, Z. P. et al. (2018), the species management in the mixed forest
523 should be carried out within the diameters of the higher CAI_v and the biological rotation
524 of the population to maximize the volume. However, we observed a large range between
525 the maximum CAI_v and the biological rotation ages, of at least 36 years and 14-cm dbh
526 (Table 3; Fig. 8). It remains unclear which MCD should be applied the highest wood
527 yield for the next cutting cycle.
528 The CAI_v curves and biological rotation ages for all species population culminated in
529 lower diameters and ages compared to the increment curves at the individual level (Fig.
530 7; Table 2). The inclusion of the number of trees per diameter class anticipates the
531 culmination since it indirectly represents the population mortality and survival rates
532 (Assmann, 1970; Rubin et al., 2006). As trees increase in size, the number of trees
533 decreases due to mortality, causing a deceleration in the gross wood production, even
534 though the remaining trees become larger (Seydack, 2000; Lundqvist, 2017). Therefore,
535 even if individual trees are growing, the total production per unit area will decline much
536 earlier (Assmann, 1970).
537 According to Seydack (2000) the population demographic factors of commercial species
538 are essential to determine the optimal parameters for forest management. In the natural
539 forest structure, the available stock of trees by diameter class is a crucial factor for yield

projection in terms of the number of trees, basal area and volume (Ong; Kleine, 1996), since they indicate survival by diameter class. The recovery time of the wood volume in a post-intervention cycle is related to the species-specific growth, and also to the number of trees in the smaller diameter classes to the intervention diameter (Brienen; Zuidema, 2006a). Therefore, methods based on the inflection point age at the population level are recognized for being more accurate in predicting maximum volume yield in a natural forest than methods that consider only the individual tree growth.

Volumetric production using different management criteria

The increments (m^3 ha^{-1} $year^{-1}$) of each species were, in general, compatible with other studies carried out in the Amazon, using permanent plots (Reis et al., 2010; Braz et al., 2018). Reis et al. (2010) obtained similar increments for *E. uncinatum* (Table 4), considering the cutting cycle and MCD of the Brazilian forest law (Brasil, 2006).

The cutting cycles and alternative MCD from those defined in Brazilian forest law produced higher volumetric increment for the 4 studied species, similar to that obtained by Groenendijk et al. (2017) in tropical rainforest in Cameroon. *Erisma uncinatum* produced approximately seven times higher wood volume (ha^{-1} $year^{-1}$) applying short cutting cycle (10 years) and MCD 70% larger (86 cm) than the Brazilian mandatory MCD (50 cm). *Erisma uncinatum* presented the highest yield gain with the alternative MCD and cutting cycles, due to the higher number of trees and growth in dbh classes above 50 cm (Fig. 2 and 7). All results, especially those of *E. uncinatum*, showed the potential of maximizing the forest management yield considering population characteristics at the species level. The ideal MCD can increase volumetric increments, even without silvicultural treatments, and so should be considered to increase management productivity (Avila et al., 2017).

564 The MCD defined by the dbh of the biological rotation of the population produced
565 higher annual increments for the four species, especially for shorter cutting cycles
566 (Table 4). It is important to consider the optimal population increment rate instead of
567 average growth data. This was previously considered by Ong and Kleine (1996) and
568 Bick et al. (1998) when studying natural forests in Malaysia. These authors obtained the
569 population growth from zero using permanent plots and simulations of forest production
570 and found the maximum sustainable yield population, defining optimum logging rates
571 and cutting cycles. Glauner et al. (2003) pointed out that the underlying principle of
572 management is to improve the forest condition, converting its stock to an optimum level
573 of increment of the commercial species.
574 In this study the dbh of the maximum CAI_v (lowest among those tested as MCD)
575 produced the lowest volume increments considering the tested cycles (Table 4).
576 According to Bick et al. (1998), the harvested volume of two cycles must oscillate in the
577 population growth curve between a lower and an upper limit of the maximum yield
578 volume (i.e., the age of maximum CAI_v). These authors recommended an MCD above
579 the dbh of maximum CAI_v. Our results are consistent with these recommendations,
580 since the yield was higher when the logging was carried out at an age after the
581 maximum population CAI_v, such as the biological rotation age.
582 When considering only the individual tree growth curve to define the logging
583 parameters we observed that the MCD was always higher, although the volumetric
584 increments were lower, except for *A. leiocarpa* (Table 4). Contrary to the statement of
585 Sebbenn et al. (2008) and Lacerda et al. (2013), the excessive MCD increase does not
586 always imply higher forest productivity for all species. As mentioned, after reaching
587 their productivity peak the trees grow at moderate rates and the mortality is high. Slow

588 growth trees should be logged before dying, through selective logging of mature trees of
589 declining vigor (Seydack, 2012; Lundqvist, 2017).
590 The cutting cycles must be long enough so that remaining trees reach the MCD
591 (Seydack et al., 1995). However, it cannot be too long, to ensure the trees' potential
592 growth and forest economic sustainability (Mattioli et al., 2015). The simulations
593 revealed that long cutting cycles resulted in smaller volumetric increments for all
594 species (Fig. 9), reaching a loss higher than 60% compared to the 10-year cutting cycle,
595 considering the same MCD (defined by population biological rotation). Therefore,
596 increasing the cutting cycle indefinitely (Sebbenn et al., 2008) represents a technical
597 error in a productive forest (Braz et al., 2015). Moreover, increasing the cut cycle
598 requires long-term investment (Glauner et al., 2003), which is difficult in unstable
599 political-economic environments (Groenendijk et al., 2017). On the other hand, short
600 cutting cycles require logging planning, following the reduced-impact logging
601 standards.
602 Suitable cutting cycles depend on economic considerations (Bick et al., 1998) besides
603 the MCD and the forest remaining structure. Economic analysis should support
604 selecting the best cutting cycle for each specific case, considering the optimal
605 parameters and exploitation feasibility for each species. Cost-benefit analyses can help
606 assess forest management's economic and social aspects (Rosa et al., 2017). Moreover,
607 higher MCD requires studies on tree health and risks of rot in older and bigger trees.
608

609 ## Conclusions

610 The diametric distribution of each species is similar throughout the transition zone
611 between open tropical rainforest and deciduous tropical rainforest in Brazilian Amazon.
612 Modifications of the standard diametric structure by species can be combined with

613 growth models for inferring tropical forest dynamics, as done in this study. The
614 diametric distribution should support wood production planning and be the basis for
615 monitoring forest logging.
616 The optimum population minimum cutting diameter (MCD) of a species can
617 significantly increase the volumetric increment and the total wood volume, maximizing
618 the forest production under management. After determining the MCD, the best cutting
619 cycle must be defined according to economic analysis, which will specify the best
620 intervention time for the productive forest.
621 The methodology for species-level MCDs proved to be a useful tool and superior to the
622 fixed parameters defined in the Brazilian law or the methodologies that consider only
623 the individual tree growth. The procedure provides higher reliability for the maximized
624 wood production. The ideal MCDs based on dendrochronology substantially reduces
625 costs and time spent collecting data for forest modeling.
626

627 ## Availability of data and materials

628 The data that support the findings of this study are available from Embrapa Florestas
629 and Elabore Projetos e Consultoria Florestal but restrictions apply to the availability of
630 these data, which were used under license for the current study, and so are not publicly
631 available. Data are however available from the authors upon reasonable request and
632 with permission of Embrapa Florestas and Elabore Projetos e Consultoria Florestal.
633

634 ## Abbreviations

635 **CAIv:** current annual volume increment
636 **DBH:** diameter at 1.30 m above ground level
637 **MAIv:** mean annual volume increment

MCD: minimum cutting diameter

PDF: probability density function

Acknowledgements

We are grateful to Elabore Projetos e Consultoria Florestal for providing inventory data and discs samples and Simon Drew for the language editing.

Funding

This work was supported by Cipem (Center of Wood Producing and Exporting Industries of Mato Grosso State), CAPES (Coordination for the Improvement of Higher Education Personnel) and Embrapa Florestas (Brazilian Agricultural Research Corporation).

Authors' contributions

AC participated of elaborating the paper conceptualization and methodology, made the formal analysis and wrote the original draft of the paper.

EMB participated of elaborating the paper conceptualization and methodology, collected field data and supervised the paper writing and design.

PPM participated of elaborating the paper conceptualization and methodology and supervised the paper writing and design.

ROB participated of elaborating the paper conceptualization and collected field data.

AFF participated of elaborating the paper conceptualization and methodology and supervised the paper writing and design.

Ethics approval and consent to participate

Not applicable

Consent for publication

Not applicable

Competing interests

The authors declare that they have no competing interests.

References

Alder D (1995) Growth Modelling for Mixed Tropical Forest, 30th edn. ODA Forestry Research programme project R4676, Oxford

Alvares CA, Stape JL, Sentelhas PC, et al (2013) Köppen's climate classification map for Brazil. Meteorol Zeitschrift 22:711–728. https://doi.org/10.1127/0941-2948/2013/0507

Amazonas (2010) Instrução Normativa no 9, de 12 de novembro de 2010. Dispõe sobre manejo florestal sustentável em áreas de várzea no Estado do Amazonas, e dá outras providências. Diário Oficial do Estado do Amazonas, Brazil

Araujo R de A, Costa RB da, Felfili JM, et al (2009) Florística e estrutura de fragmento florestal em área de transição na Amazônia Matogrossense no município de Sinop. Acta Amaz 39:865–877. https://doi.org/10.1590/S0044-59672009000400015

Assmann E (1970) The principles of forest yield study. Pergamon Press Ltd.

684 Avila AL, Schwartz G, Ruschel AR, et al (2017) Recruitment, growth and recovery of
685 commercial tree species over 30 years following logging and thinning in a tropical
686 rain forest. For Ecol Manage 385:225–235.
687 https://doi.org/10.1016/j.foreco.2016.11.039

688 Bailey RL, Dell R (1973) Quantifying Diameter Distributions with the Weibull
689 Function. For Sci 19:97–104

690 Bettinger P, Boston K, Siry J, Grebner D (2009) Forest Management and Planning.
691 Academic Press, New York

692 Bick U, Droste H-J, Glauner R, Heuveldop JO (1998) Assessment and measurement of
693 forestry key parameters for the evaluation of tropical forest management. Plant Res
694 Dev 47/48:38–61

695 Brasil (2006) Instrução normativa n. 6 de 11 de dezembro de 2006. Diário Oficial da
696 União, Brasília, DF, 13 dez. 2006. Seção 1, p. 155

697 Braz EM, Mattos PP (2015) Manejo De Produção Em Florestas Naturais Da Amazônia:
698 Mitos E Verdades. Nativa 3:292–295. https://doi.org/10.14583/2318-
699 7670.v03n04a12

700 Braz EM (2010) Subsídios para o planejamento do manejo de florestas tropicais da
701 amazônia. Universidade Federal de Santa Maria

702 Braz EM, Canetti A, Mattos PP, et al (2018) Alternative criteria to achieve sustainable
703 management of Mezilaurus itauba in the Brazilian Amazon. Pesqui Florest Bras
704 38:1–8. https://doi.org/10.4336/2018.pfb.38e201801648

Braz EM, Mattos PP de, Oliveira MF, Basso RO (2014) Strategies for Achieving Sustainable Logging Rate in the Brazilian Amazon Forest. Open J For 04:100–105. https://doi.org/10.4236/ojf.2014.42015

Braz EM, Mattos PP, Thaines F, et al (2015) Criteria to be considered to achieve a sustainable second cycle in Amazon Forest. Pesqui Florest Bras 35:209. https://doi.org/10.4336/2015.pfb.35.83.941

Brienen RJW (2005) Tree rings in the tropics: a study on growth and ages of Bolivian rain forest trees

Brienen RJW, Zuidema PA (2006) The use of tree rings in tropical forest management : Projecting timber yields of four Bolivian tree species. For Ecol Manage 226:256–267. https://doi.org/10.1016/j.foreco.2006.01.038

Brienen RJW, Zuidema PA (2006) Lifetime growth patterns and ages of Bolivian rain forest trees obtained by tree ring analysis. J Ecol 94:481–493. https://doi.org/10.1111/j.1365-2745.2005.01080.x

Burkhart HE, Tomé M (2012) Modeling Forest Trees and Stands. Springer Netherlands, Dordrecht

Canetti A, de Mattos PP, Braz EM, Netto SP (2017) Life pattern of urban trees: A growth-modelling approach. Urban Ecosyst 20:1057–1068

Carvalho PER (1981) Competição entre espécies florestais nativas em Irati - PR, cinco anos após o plantio. Bol Pesqui Florest 41–56

725 Clark D a., Clark DB (1992) Life history diversity of canopy and emergent trees in a
726 neotropical rain forestClark, D. A. ., & .C. and D. B. (1992). Life history diversity
727 of canopy and emergent trees in a neotropical rain forest. Ecological monographs,
728 62(3), 315-344. Retrieved from. Ecol Monogr 62:315–344.
729 https://doi.org/10.2307/2937114

730 Condit R, Sukumar R, Hubbell SSP, et al (1998) Predicting Population Trends from
731 Size Distributions : A Direct Test in a Tropical Tree Community. Am Nat
732 152:495–509. https://doi.org/10.1086/286186

733 Coomes DA, Duncan RP, Allen RB, Truscott J (2003) Disturbances prevent stem size-
734 density distributions in natural forests from following scaling relationships. Ecol
735 Lett 6:980–989. https://doi.org/10.1046/j.1461-0248.2003.00520.x

736 Dawkins HC, Philip MS (1998) Tropical Moist Forest Silviculture and Management: A
737 History of Success and Failure. CAB International, Wallingford, UK

738 de Liocourt F (1898) De l'amenagement des sapinières. Bull Trimest 396–409

739 Dionisio LFS, Schwartz G, Lopes J do C, Oliveira F de A (2018) Growth, mortality,
740 and recruitment of tree species in an Amazonian rainforest over 13 years of
741 reduced impact logging. For Ecol Manage 430:150–156.
742 https://doi.org/10.1016/j.foreco.2018.08.024

743 D'Oliveira MVN, Oliveira LC, Acuña MHA, Braz EM (2017) Twenty years monitoring
744 growth dynamics of a logged tropical forest in Western Amazon. Pesqui Florest
745 Bras 37:493–502. https://doi.org/10.4336/2017.pfb.37.92.1398

746 Felfili JM (1997) Diameter and height distributions in a gallery forest tree community
747 and some of its main species in central Brazil over a six-year period (1985-1991).
748 Rev Bras Botânica 20:155–162. https://doi.org/10.1590/S0100-
749 84041997000200006

750 Fortini LB, Zarin DJ (2011) Population dynamics and management of Amazon tidal
751 floodplain forests: Links to the past, present and future. For Ecol Manage 261:551–
752 561. https://doi.org/10.1016/j.foreco.2010.11.007

753 Fortini LB, Cropper WP, Zarin DJ (2015) Modeling the complex impacts of timber
754 harvests to find optimal management regimes for Amazon tidal floodplain forests.
755 PLoS One 10:1–18. https://doi.org/10.1371/journal.pone.0136740

756 Free CM, Grogan J, Schulze MD, et al (2017) Current Brazilian forest management
757 guidelines are unsustainable for Swietenia, Cedrela, Amburana, and Copaifera: A
758 response to da Cunha and colleagues. For Ecol Manage 386:81–83.
759 https://doi.org/10.1016/j.foreco.2016.09.031

760 Free CM, Matthew Landis R, Grogan J, et al (2014) Management implications of long-
761 term tree growth and mortality rates: A modeling study of big-leaf mahogany
762 (Swietenia macrophylla) in the Brazilian Amazon. For Ecol Manage 330:46–54.
763 https://doi.org/10.1016/j.foreco.2014.05.057

764 Glauner R, Ditzer T, Huth A (2003) Growth and yield of tropical moist forest for forest
765 planning: an inquiry through modeling. Can J For Res 33:521–535.
766 https://doi.org/10.1136/bmj.2.2867.854

767 Gotelli NJ (2008) A Primer of Ecology. Sinauer Associates Inc., Sunderland,
768 Massachusetts

769 Gouveia D, Soares M, Silva W, et al (2011) Avaliação do crescimento de espécies
770 florestais por grupo ecológico em áreas exploradas na FLONA do Tapajós. III
771 Encontro Amaz Agrárias 1–5

772 Groenendijk P, Bongers F, Zuidema PA (2017) Using tree-ring data to improve timber-
773 yield projections for African wet tropical forest tree species. For Ecol Manage
774 400:396–407. https://doi.org/10.1016/j.foreco.2017.05.054

775 Higuchi N (1996) Utilização e manejo dos recursos madeireiros das florestas tropicais
776 úmidas. Acta Amaz 24:275–288

777 Hossain MA, Hossain MK, Alam MS, Uddin MM (2015) Composition and Diversity of
778 Tree Species in Kamalachari Natural Forest of Chittagong South Forest Division,
779 Bangladesh. J For Environ Sci 31:192–201.
780 https://doi.org/10.7747/JFES.2015.31.3.192

781 IBGE - Instituto Brasileiro de Geografia e Estatística (1992) Mapa de vegetação do
782 Brasil -Escala 1:5.000.000. http://www.dpi.inpe.br/Ambdata/mapa_sipam.php.
783 Accessed 10 Mar 2017

784 IBGE - Instituto Brasileiro de Geografia e Estatística (2010) Censo Demográfico.
785 https://censo2010.ibge.gov.br. Accessed 11 Nov 2017

786 Kohyama T (1986) Tree size structure of stands and each species in primary warm-
787 temperate rain forests of Southern Japan. Bot Mag Tokyo 99:267–279.
788 https://doi.org/10.1007/BF02489543

789 Lacerda AEB, Nimmo ER, Sebbenn AM (2013) Demography of Hymenaea courbaril.
790 For Sci 59:15–26

791 Lamprecht H (1990) Silvicultura nos tropicos: ecossistemas florestais e respectivas
792 especies arboreas - possibilidades e metodos de aproveitamento sustentado. GTZ,
793 Eschborn

794 Lanssanova LR (2012) Ajuste De Funções De Afilamento Para Espécies Florestais
795 Comerciais Do Bioma Amazônico Matogrossense. Universidade Federal do Mato
796 Grosso - UFMT

797 Lanssanova LR, Silva FA da, Schons CT, Pereira ACDS (2018) Comparação Entre
798 Diferentes Métodos Para Estimativa Volumétrica De Espécies Comerciais Da
799 Amazônia. BIOFIX Sci J 3:109–115. https://doi.org/10.5380/biofix.v3i1.57489

800 Lappi J (1997) A Longitudinal Analysis of Height / Diameter Curves HEIGHT PLAYS
801 TWO in modeling the growth. For Sci 43:555–570

802 Larson BC (1992) Pathways of development in mixed-species stands. In: Kelty MJ,
803 Larson BC, Oliver CD (eds) The Ecology and Silviculture of Mixed-Species
804 Forests. Springer, Dordrecht, Netherlands, pp 3–10

805 Lundqvist L (2017) Tamm Review: Selection system reduces long-term volume growth
806 in Fennoscandic uneven-aged Norway spruce forests. For Ecol Manage 391:362–
807 375. https://doi.org/10.1016/j.foreco.2017.02.011

808 Maciel MDNM, Watzlawick LF, Schoeninger ER, Yamaji FM (2017) Classificação
809 ecológica das espécies arbóreas. Rev Acadêmica Ciência Anim 1:69.
810 https://doi.org/10.7213/cienciaanimal.v1i2.14922

811 Madron LD De, Forni E (1997) Aménagement forestier dans l'Est du Cameroun. Bois
812 Forêts des Trop 39–50. https://doi.org/https://agritrop.cirad.fr/389267

813 Mattioli W, Ferrari B, Giuliarelli D, et al (2015) Conversion of Mountain Beech
814 Coppices into High Forest: An Example for Ecological Intensification. Environ
815 Manage 56:1159–1169. https://doi.org/10.1007/s00267-015-0549-2

816 Mattos PP, Braz EM, Domene VD, et al (2015) Relação Clima-Crescimento De Árvores
817 De Mimosa Tenuiflora Em Floresta Tropical Seca Sazonal, Brazil. Cerne 21:141–
818 149. https://doi.org/10.1590/01047760201521011460

819 Meyer HA (1952) Balanced Growth , and Drain in Uneven-Aged Forests. J For

820 Miller DP (2004) Bootstrap 101: Obtain robust confidence intervals for any statistic. In:
821 Twenty-Ninth Annual SAS Users Group International Conference. SAS Institute,
822 Cary, NC, pp 193–29

823 Miranda DLC, Higuchi N, Trumbore SE, et al (2018) Using radiocarbon-calibrated
824 dendrochronology to improve tree-cutting cycle estimates for timber management
825 in southern Amazon forests. Trees - Struct Funct 32:587–602.
826 https://doi.org/10.1007/s00468-018-1658-3

827 Miranda ZP, Guedes MC, Rosa SA, Schöngart J (2018) Volume increment modeling
828 and subsidies for the management of the tree Mora paraensis (Ducke) Ducke based
829 on the study of growth rings. Trees - Struct Funct 32:277–286.
830 https://doi.org/10.1007/s00468-017-1630-7

831 Muller-Landau HC, Condit RS, Harms KE, et al (2006) Comparing tropical forest tree
832 size distributions with the predictions of metabolic ecology and equilibrium
833 models. Ecol Lett 9:589–602. https://doi.org/10.1111/j.1461-0248.2006.00915.x

834 Nyland RD (2002) Silviculture: concepts and applications, 2nd edn. McGraw-Hill,
835 Boston, MA

836 Odum EP (1988) Ecologia, Guanabara. Rio de Janeiro, Brasil

837 O'Hara K (2014) Transformations to Multiaged Stand Structures. In: Multiaged
838 Silviculture: Managing for Complex Forest Stand Structures. Oxford University
839 Press, pp 1–15

840 Oliveira MF, Braz EM, Mattos PP de, et al (2015) Padrão de crescimento e diâmetro
841 ótimo de corte de cupiúba na microrregião de Sinop, MT. Colombo, Brasil

842 Oliver CD (1992) Similarities of stand structures and stand development processes
843 throughout the world—some evidence and applications to silviculture through
844 adaptive management. In: Kelty MJ, Larson BC, Oliver CD (eds) The Ecology and
845 Silviculture of Mixed-Species Forests. Springer, Dordrecht, Dordrecht,
846 Netherlands, pp 11–26

847 Ong RC, Kleine M (1996) DIPSIM: Dipterocarp forest growth simulation model--a tool
848 for forest-level management planning. Dipterocarp For Ecosyst Sustain Manag
849 World Sci Singapore 228–246. https://doi.org/10.1017/CBO9781107415324.004

850 Orellana E, Figueiredo Filho A (2017) Uso do método da predição de parâmetros para
851 projetar a distribuição diamétrica em florestas nativas com a função Weibull.
852 Ciência Florest 27:981–991

853 Pascal J (2003) Notions sur les structure et dynamique des forêts tropicales humides.
854 Rev For Française 118. https://doi.org/10.4267/2042/5765

855 Reis LP, Ruschel AR, Coelho AA, et al (2010) Avaliação do potencial madeireiro na
856 Floresta Nacional do Tapajós após 28 anos da exploração florestal. Pesqui Florest
857 Bras 30:265–281. https://doi.org/10.4336/2010.pfb.30.64.265

858 Reynolds MR, Burk TE, Huang W-C (1988) Goodness-of-Fit Tests and Model
859 Selection Procedures for Diameter Distribution Models. For Sci 34:373–399

860 Ribeiro ES, Paula MH De, Rossi R, et al (2016) Espécies florestais comercializadas
861 pelo estado de mato grosso. Biodiversidade 15:2–20

862 Rinn F (1996) TSAP Win v. 3.6: Reference Manual: Computer Program for Tree-Ring
863 Analysis and Presentation. RINNTECH, Heidelberg, Germany

864 Rosa SA, Barbosa ACMC, Junk WJ, et al (2017) Growth models based on tree-ring data
865 for the Neotropical tree species Calophyllum brasiliense across different Brazilian
866 wetlands: implications for conservation and management. Trees - Struct Funct
867 31:729–742. https://doi.org/10.1007/s00468-016-1503-5

868 Rubin BD, Manion PD, Faber-Langendoen D (2006) Diameter distributions and
869 structural sustainability in forests. For Ecol Manage 222:427–438.
870 https://doi.org/10.1016/j.foreco.2005.10.049

871 Schaaf LB, Figueiredo Filho A, Galvão F, Sanquetta CR (2006) Alteração na estrutura
872 diamétrica de uma floresta ombrófila mista no período entre 1979 e 2000. Rev
873 Árvore 30:283–295. https://doi.org/10.1590/S0100-67622006000200016

874 Schöngart J (2011) Amazonian Floodplain Forests. Springer Netherlands, Dordrecht

875 Schöngart J (2008) Growth-Oriented Logging (GOL): A new concept towards
876 sustainable forest management in Central Amazonian várzea floodplains. For Ecol
877 Manage 256:46–58. https://doi.org/10.1016/j.foreco.2008.03.037

878 Scolforo J (1998) Manejo florestal. Lavras: UFLA/FAEPE 1158–1170

879 Sebbenn AM, Degen B, Azevedo VCR, et al (2008) Modelling the long-term impacts of
880 selective logging on genetic diversity and demographic structure of four tropical
881 tree species in the Amazon forest. For Ecol Manage 254:335–349.
882 https://doi.org/10.1016/j.foreco.2007.08.009

883 Seydack AHW (2012) Regulation of Timber Yield Sustainability for Tropical and
884 Subtropical Moist Forests: Ecosilvicultural Paradigms and Economic Constraints.
885 In: Continuous Cover Forestry. Managing Forest Ecosystems. Springer, Dordrecht,
886 pp 129–165

887 Seydack AHW (2000) Theory and Practice of Yield Regulation Systems for Sustainable
888 Management of Tropical and Subtropical Moist Natural Forests. In: von Gadow K,
889 Pukkala T, Tomé M (eds) Sustainable Forest Management. Springer Netherlands,
890 Dordrecht, pp 257–318

891 Seydack AHW, Vermeulen WJ, Heyns HE, et al (1995) An unconventional approach to
892 timber yield regulation for multi-aged, multispecies forests. II. Application to a
893 South African forest. For Ecol Manage 77:155–168. https://doi.org/10.1016/0378-
894 1127(95)03578-X

895 Silva JNM (1989) The behavior of the tropical rain forest of the Brazilian amazon after
896 logging. Oxford University

897 Silva JNM (1997) Manejo de florestas de terra-firme da Amazônia Brasileira. In:
898 Tópicos em manejo florestal sustentável. Embrapa Florestas, Colombo, pp 59–96

899 Silva JNM, Carvalho JOP de, Lopes J do CA (1985) Inventário florestal de uma área
900 experimental na Floresta Nacional do Tapajós. Bol Pesqui Florest 38–110

901 SIVAM P (2002) Mapa de Vegetação da Amazônia Legal – RADAM/SIPAM. In:
902 DNPM, Ministério Minas e Energ.
903 http://www.dpi.inpe.br/Ambdata/mapa_sipam.php. Accessed 10 Mar 2018

904 van Gardingen PR, Valle D, Thompson I (2006) Evaluation of yield regulation options
905 for primary forest in Tapajós National Forest, Brazil. For Ecol Manage 231:184–
906 195. https://doi.org/10.1016/j.foreco.2006.05.047

907 Vanclay JK (1989) A growth model for north Queensland rainforests. For Ecol Manage
908 27:245–271. https://doi.org/10.1016/0378-1127(89)90110-2

909 Wang X, Hao Z, Zhang J, et al (2009) Tree size distributions in an old-growth
910 temperate forest. Oikos 118:25–36. https://doi.org/10.1111/j.1600-
911 0706.2008.16598.x

912 Wright SJ, Muller-Landau HC, Condit R, Hubbell SP (2003) Shade tolerance, realized
913 vital rates, and size distributions of tropical trees. Ecology 84:3174–3185

914 Yegang W, Jinxuan H (1988) A Spectral Analysis of the Population Dynamics of
915 Korean Pine in the Mixed Broad-leaved Pinus koraiensis Forest. J Ecol 19–23

Figures

Obtained from:

Pdf	Dbh growth equation	Taper equations	N x v		Derivatives of V	
N (trees ha^{-1})	**Time (years)**	**Dbh (cm)**	**v (m^3)**	**V (m^3 ha^{-1})**	**MAIv (m^3 ha^{-1} year^{-1})**	**CAIv (m^3 ha^{-1} year^{-1})**
0.0955	70	27.8696	0.3783	0.0361	5.16×10^{-4}	1.86×10^{-3}
0.0957	71	28.4297	0.3971	0.0380	5.35×10^{-4}	1.88×10^{-3}
0.0958	72	28.9951	0.4166	0.0399	5.54×10^{-4}	1.91×10^{-3}
0.0958	73	29.5656	0.4368	0.0419	5.73×10^{-4}	1.93×10^{-3}
0.0957	74	30.1413	0.4577	0.0438	5.92×10^{-4}	1.95×10^{-3}
0.0955	75	30.7221	0.4793	0.0458	6.10×10^{-4}	1.97×10^{-3}

Figure 1

Scheme showing the methodological process for obtaining the curves of volume increment of the population. The boxes with red outline inform the data source of the column to which the arrows are directed. PDFs = probability density functions; N = number of trees per hectare; dbh = diameter at 1.30 m above ground level; v = volume of individual tree; V = species population volume (m³ ha-1); MAIv = mean annual volume increment; and CAIv = current annual volume increment.

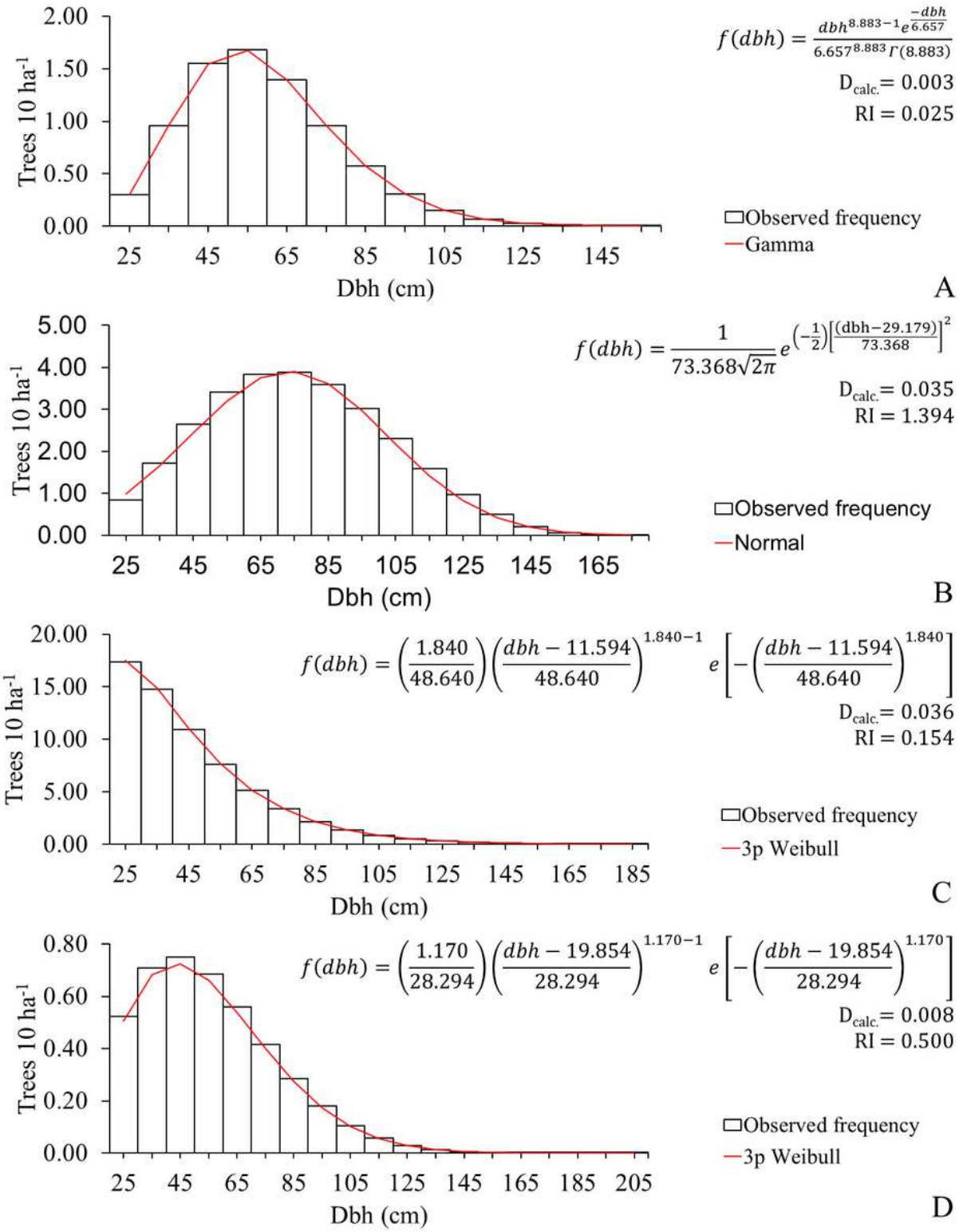

Figure 2

Probability density functions with better fitting for Apuleia leiocarpa (A), Erisma uncinatum (B), Hymenolobium excelsum (C) and Trattinnickia burserifolia (D). Dbh = diameter at 1.30 m above ground level (cm); Γ = gamma function; Dcalc. = maximum absolute value between fitted pdf and observed values in each compartment; IR = error index (Reynolds et al., 1988).

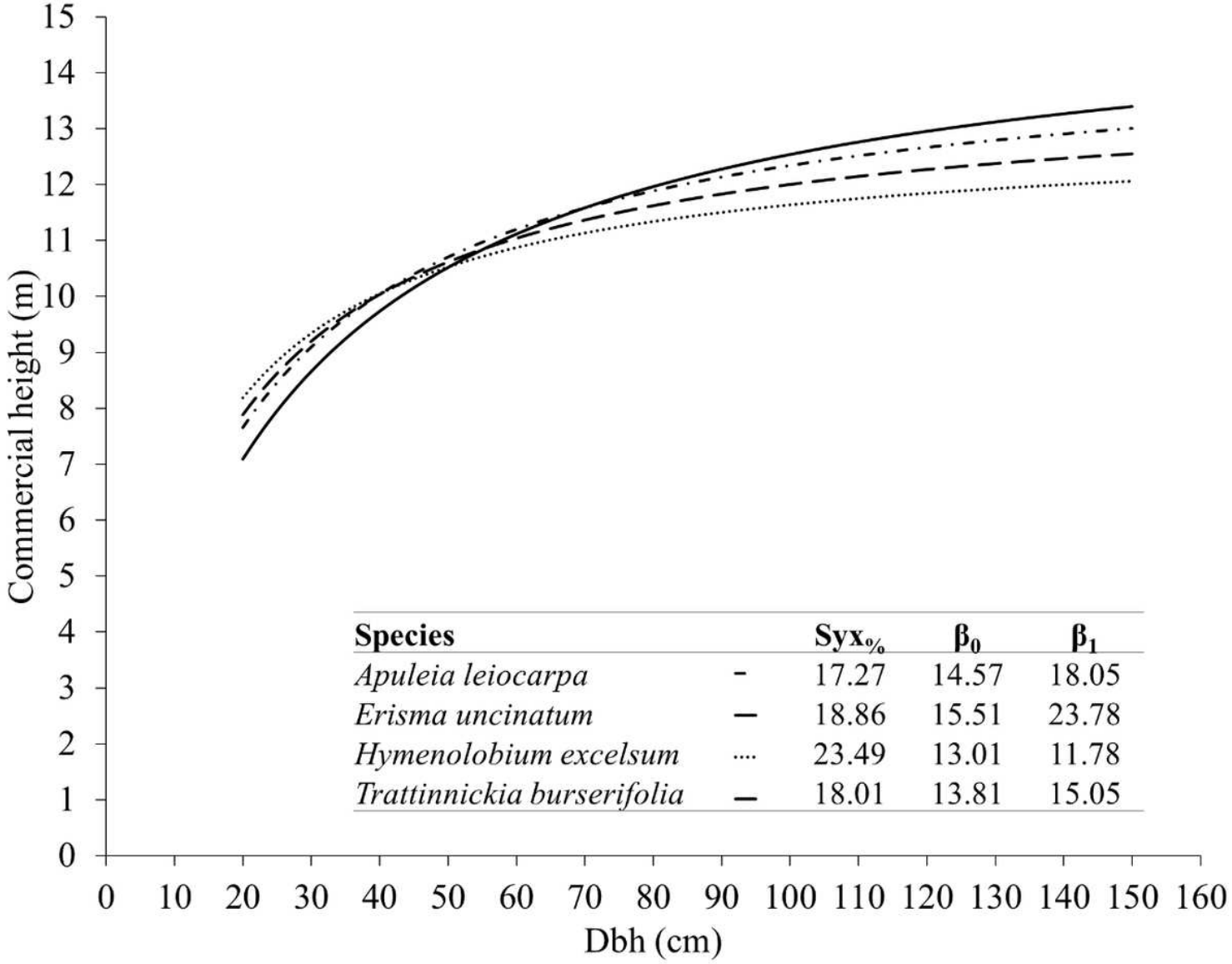

Figure 3

Heigh/dbh models of Apuleia leiocarpa, Erisma uncinatum, Hymenolobium excelsum, and Trattinnickia burserifolia. dbh = diameter at 1.30 m above ground level (cm); β0 and β1 = equation parameters fitted by non-linear regression; Syx% = relative residual standard error (%)

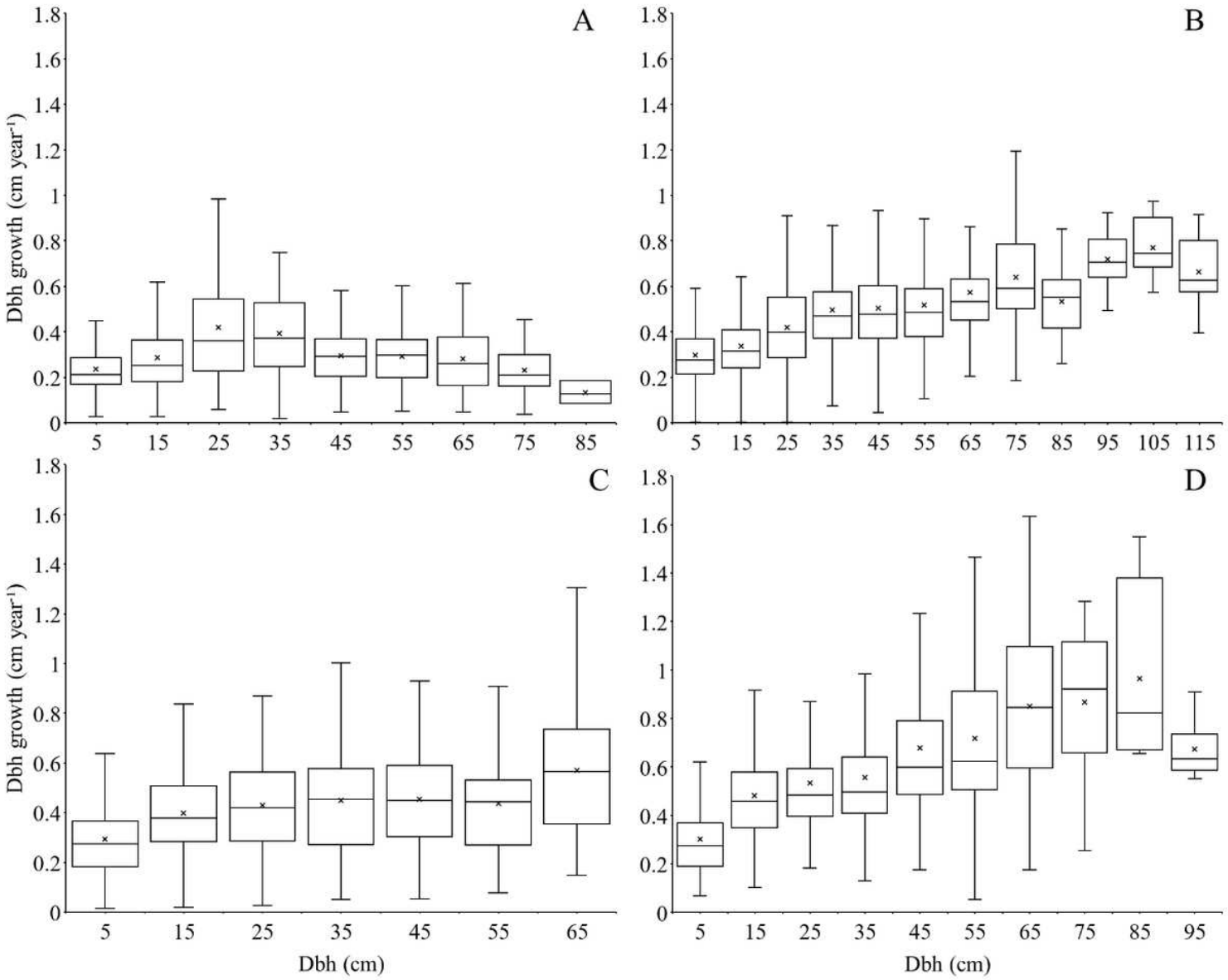

Figure 4

Boxplot of the mean annual periodic increment by diameter class of Apuleia leiocarpa (A), Erisma uncinatum (B), Hymenolobium excelsum (C), and Trattinnickia burserifolia (D). Markers (x) represent the mean increment per diameter class, which were calculated only for the diameter classes with three or more trees. Dbh = diameter at 1.30 m above ground level.

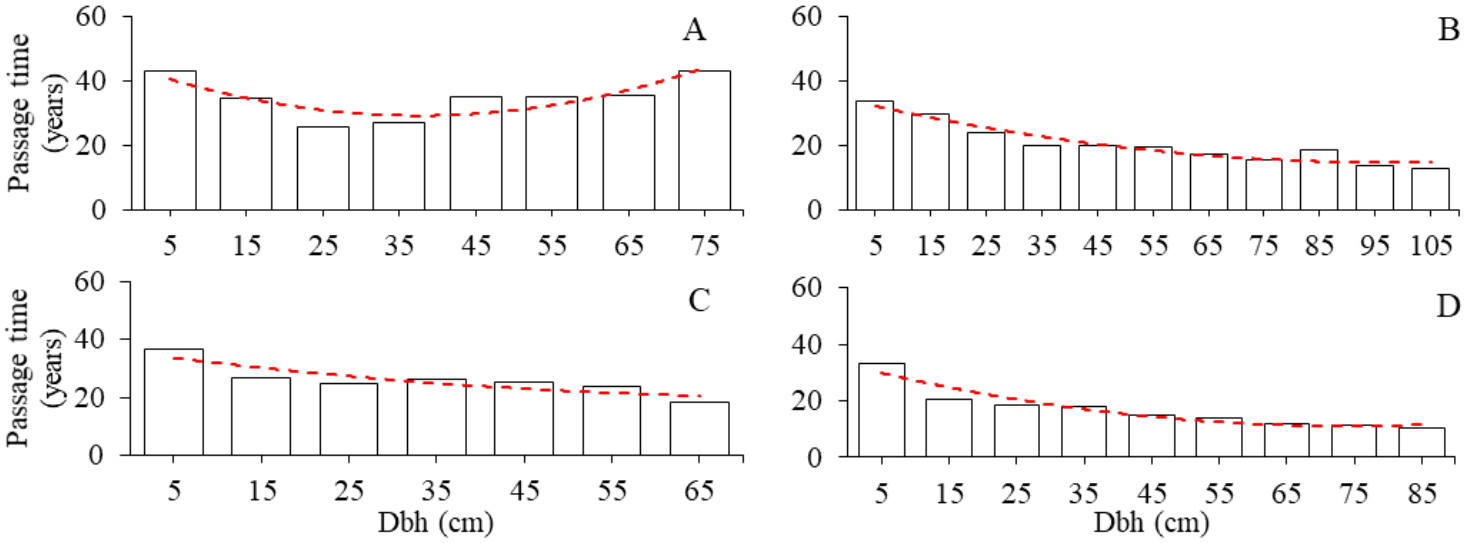

Figure 5

Mean passage time by diameter class for Apuleia leiocarpa (A), Erisma uncinatum (B), Hymenolobium excelsum (C), and Trattinnickia burserifolia (D) and their respective tendency lines. Only passage times for diameter classes with three or more trees were considered. Dbh = diameter at 1.30 m above ground level.

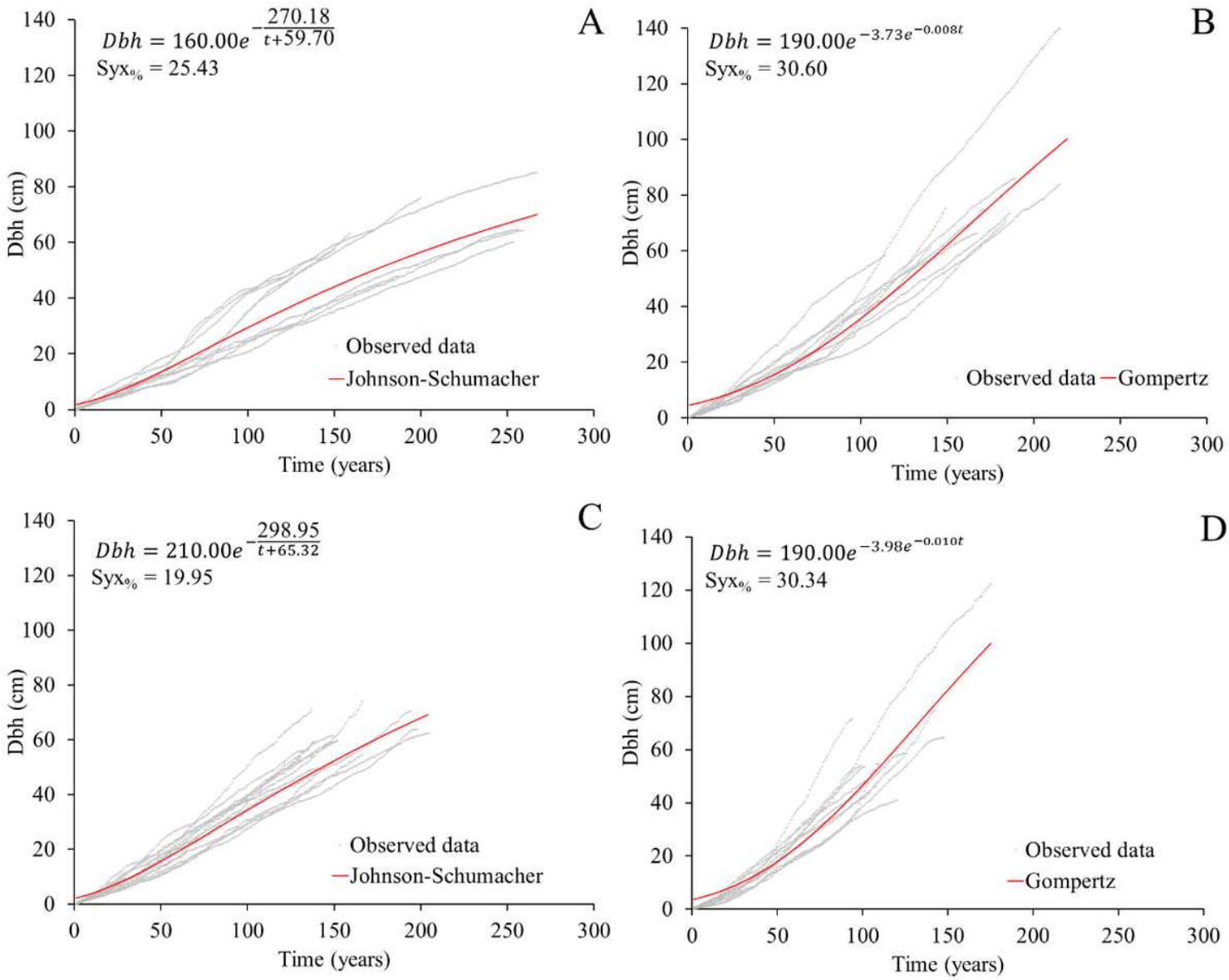

Figure 6

Accumulated diametric growth equations fitted for Apuleia leiocarpa (A), Erisma uncinatum (B), Hymenolobium excelsum (C), and Trattinnickia burserifolia (D). The growth equations were fitted for the ages represented by three or more samples. Dbh = diameter at 1.30 m above ground level; t = time (years); Syx% = Relative Residual Standard Error (%).

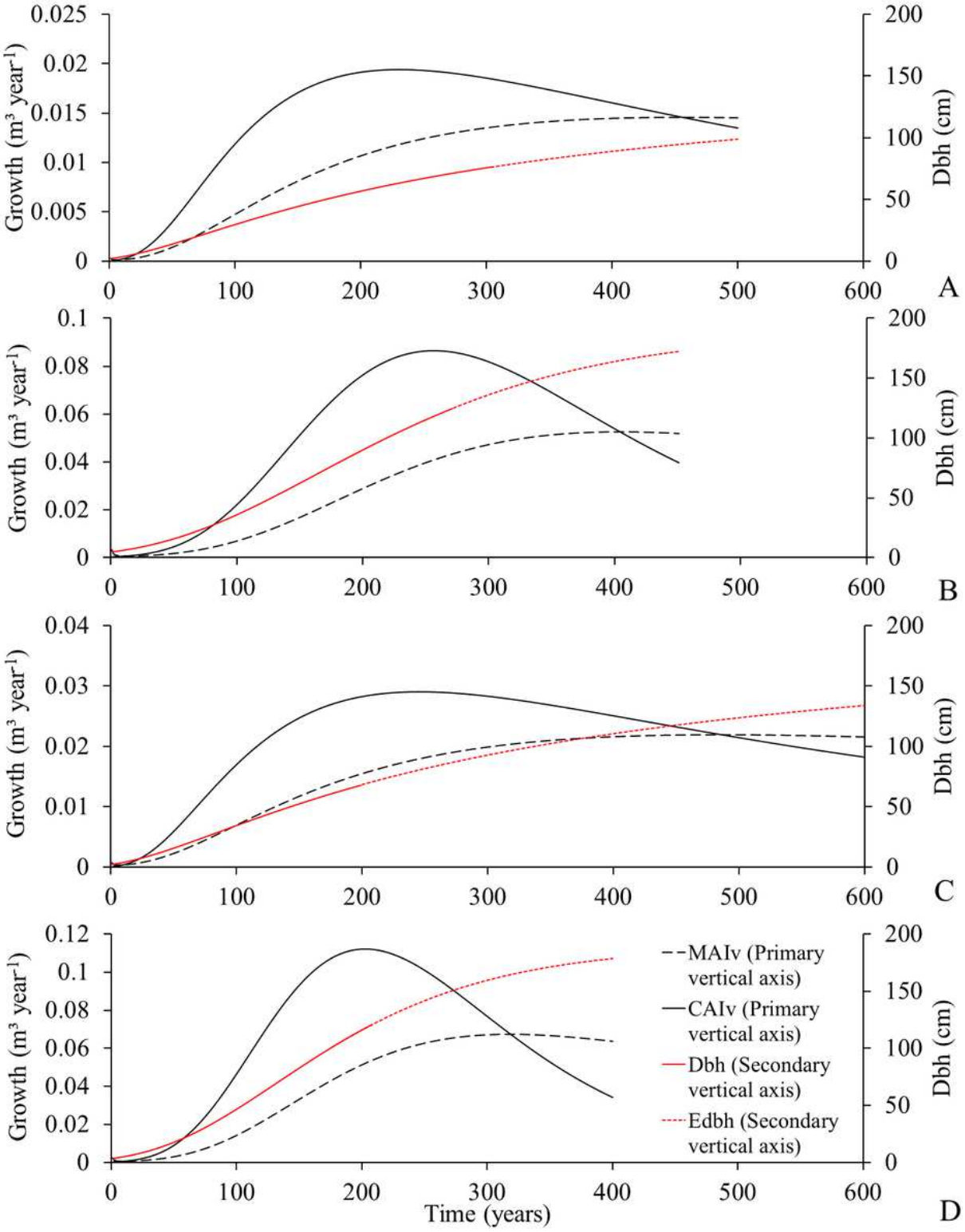

Figure 7

Volumetric increment curves (black) and dbh growth equation (red) for Apuleia leiocarpa (A), Erisma uncinatum (B), Hymenolobium excelsum (C), and Trattinnickia burserifolia (D). In the primary y-axis: MAIv = mean annual volumetric increment; CAIv = current annual volumetric increment. On the secondary y-axis: dbh = diameter at 1.30 m above ground level (cm) (growth equation fitted within the measured data

range); Edbh = accumulated diameter at 1.30 m above ground level (growth equation outside the measured data range).

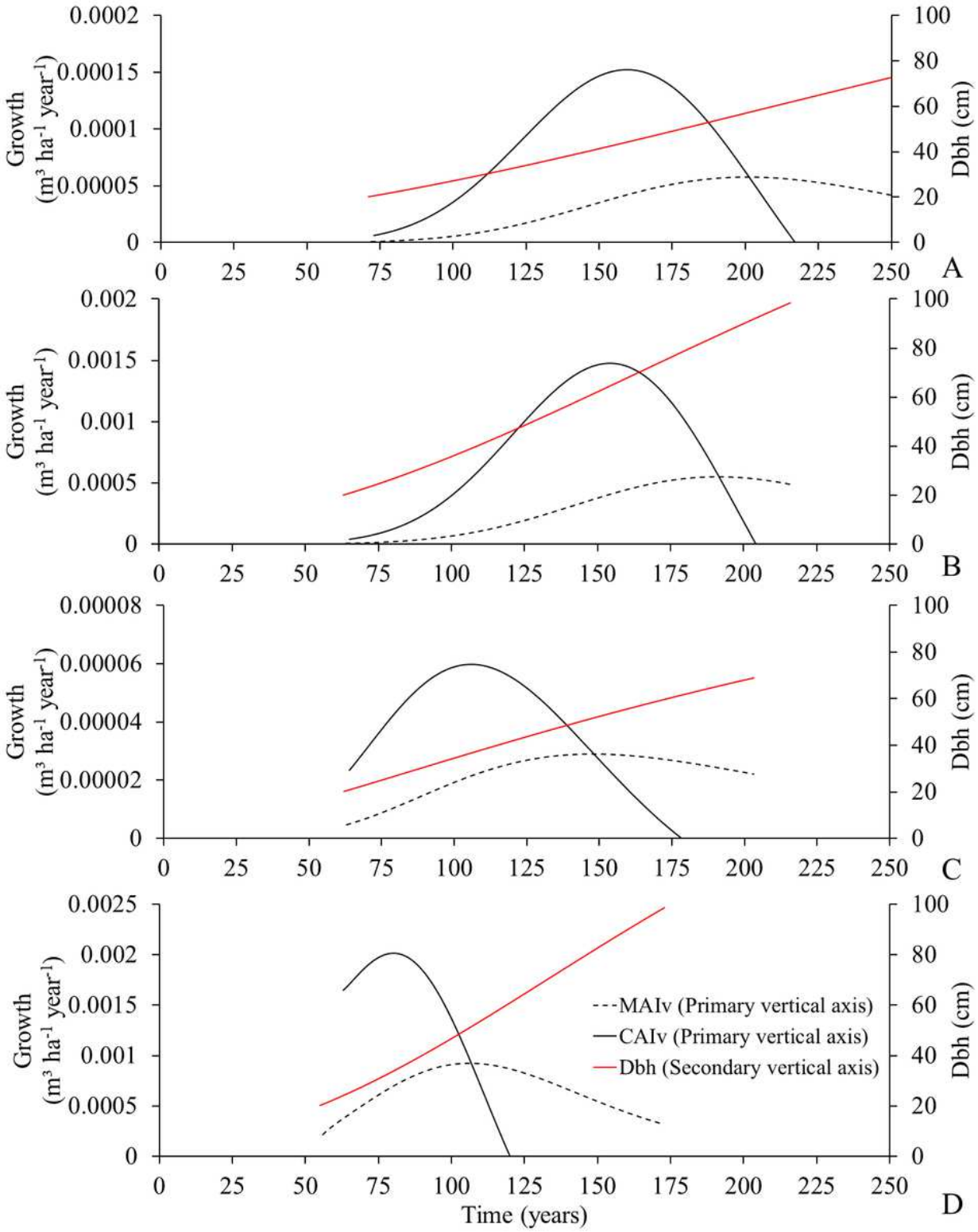

Figure 8

Volumetric and diametric increment curves for the population of Apuleia leiocarpa (A), Erisma uncinatum (B), Hymenolobium excelsum (C) and Trattinnickia burserifolia (D) (dbh ≥ 20 cm). In the primary y-axis:

MAIv = mean annual increment in volume; CAIv = current annual increment in volume. In the secondary y-axis: dbh = diameter at 1.30 m above ground level (cm), obtained from the growth equation.

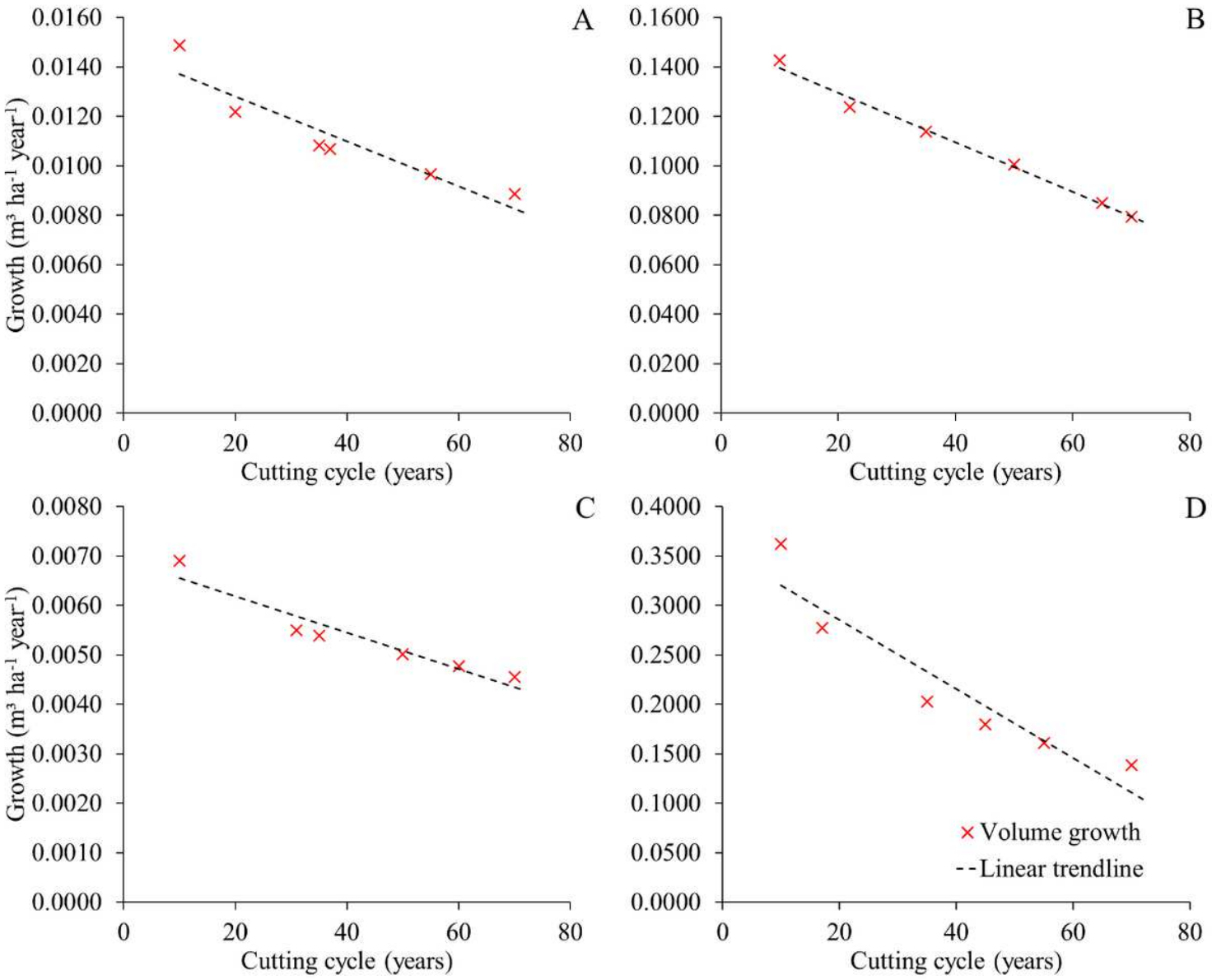

Figure 9

Annual volume increment by the MCD defined by the population's biological rotation age and different cutting cycles for Apuleia leiocarpa (A), Erisma uncinatum (B), Hymenolobium excelsum (C), and Trattinnickia burserifolia (D).